Optical water quality in rivers

J. P. Julian,[1,2] M. W. Doyle,[1] S. M. Powers,[3] E. H. Stanley,[3] and J. A. Riggsbee[4]

Received 20 August 2007; revised 11 June 2008; accepted 23 July 2008; published 18 October 2008.

[1] Optical water quality (OWQ) governs the quantity and quality of light in aquatic ecosystems, and thus spatiotemporal changes in OWQ affect many biotic and abiotic processes. Despite the fundamental role of light in rivers, studies on riverine OWQ have been limited and mostly descriptive. Here we provide a comprehensive, quantitative analysis of the controls and spatiotemporal dynamics of riverine OWQ, focusing on the inherent optical properties (IOPs), which are those that are only affected by water constituents and not by changes in the solar radiation field. First, we briefly review the constituents attenuating light in rivers. Second, we develop a new method for partitioning (light) beam attenuation into its constituent fractions. This method distinguishes between absorption and scattering by dissolved and particulate constituents, and further isolates particulates into mineral and organic components. Third, we compare base flow IOPs between four rivers with vastly different physical characteristics to illustrate intersite variability. Fourth, we analyze the spatial and temporal patterns of IOPs for the four rivers. Fifth, we quantify a longitudinal water clarity budget for one of the rivers. Finally, available data are synthesized to identify general spatial trends robust across broad geographic areas. Temporal trends in IOPs were largely dictated by storm frequency, while spatial trends were largely dictated by channel network configuration. Generally, water clarity decreased with increasing discharge primarily owing to greater scattering by particulates and secondarily to greater absorption by chromophoric dissolved organic matter. Water clarity also generally decreased longitudinally along the river owing to increased particulate inputs from tributaries; however, for pear-shaped, dendritic basins, water clarity reached a minimum at ~70% of the channel length and then increased. By illustrating the controls and spatiotemporal variability of riverine OWQ, these findings will be of interest to water resource managers and fluvial ecologists and specifically for remote-sensing of fluvial environments and river plumes in receiving waters.

Citation: Julian, J. P., M. W. Doyle, S. M. Powers, E. H. Stanley, and J. A. Riggsbee (2008), Optical water quality in rivers, *Water Resour. Res.*, *44*, W10411, doi:10.1029/2007WR006457.

1. Introduction

[2] Optical water quality (OWQ) has been defined as "the extent to which the suitability of water for its functional role in the biosphere or the human environment is determined by its optical properties" [*Kirk*, 1988]. Accordingly, OWQ governs the behavior of photons in aquatic ecosystems and determines underwater light quantity (number of photons) and quality (spectral distribution). It therefore influences primary productivity, water temperature, faunal movements, photodegradation of organic matter, and numerous other photoassisted biogeochemical reactions [*Wetzel*, 2001]. Changes in OWQ can indicate important environmental trends such as eutrophication, sedimentation, or general water quality degradation. Additionally, OWQ is a key component of aesthetics, recreation, and management of water resources [*Davies-Colley et al.*, 2003]. Thus, OWQ reflects prevailing environmental conditions and dictates multiple aspects of ecosystem structure and function.

[3] The significance of light has long been recognized in oceans, estuaries, and lakes, but has usually been ignored and at most dealt with in a descriptive, qualitative fashion in rivers. Of the body of work that exists on rivers, most address only individual influences such as light attenuation by sediments. Further, the high variability and difficulty of characterization of riverine OWQ [*Davies-Colley et al.*, 2003] has delayed a comprehensive understanding. The lack of information persists despite the central role ascribed to light availability in fluvial ecology models such as the River Continuum Concept (RCC; *Vannote et al.* [1980]). Nonetheless, the eclectic nature of OWQ and the ease of field measurement has resulted in its adoption as a water quality standard in some countries [*Davies-Colley et al.*, 2003].

[4] The goal of this paper is to provide a comprehensive overview of the spatial and temporal dynamics of riverine

[1]Department of Geography, University of North Carolina, Chapel Hill, North Carolina, USA.
[2]Now at Department of Geography, University of Oklahoma, Norman, Oklahoma, USA.
[3]Center for Limnology, University of Wisconsin, Madison, Wisconsin, USA.
[4]Department of Environmental Sciences and Engineering, University of North Carolina, Chapel Hill, North Carolina, USA.

0043-1397/08/2007WR006457$09.00

OWQ, focusing on the inherent optical properties (IOPs); those that are only affected by water constituents and not by changes in the solar radiation field. First, the constituents influencing IOPs are briefly reviewed. Second, a new method is developed for partitioning light beam attenuation into its constituent fractions. Third, we compare base flow IOPs between four rivers with vastly different physical characteristics to illustrate intersite variability. Fourth, we analyze the spatial and temporal distributions of IOPs for the four rivers. Fifth, we quantify a water clarity budget for one of the rivers, including tributary inputs. Finally, available data are synthesized to identify general spatial trends robust across broad geographic areas. Throughout the paper, we place our findings in the context of prevailing fluvial ecosystem theory.

2. Components of Optical Water Quality

[5] When light enters water, it interacts with dissolved and particulate substances by the processes of absorption and scattering. Although light is mostly lost through absorption, scattering can be a major influence on the quantity of light because it increases the probability of absorption [*Kirk*, 1994]. Absorption influences the quality of light by selectively removing photons with specific wave bands. The absolute quantities of scattering and absorption are expressed by an absorption coefficient (a) and a scattering coefficient (b), which respectively are the fraction of radiant flux (light per time) that is absorbed and scattered by an infinitesimally thin layer of aquatic medium per unit distance along the light path. Together, a and b establish the (light) beam attenuation coefficient (c), the fraction of radiant flux that is lost over the infinitesimally thin layer of aquatic medium, in m^{-1}:

$$c = a + b \tag{1}$$

This value of c is closely and inversely related to the visual clarity of water [*Davies-Colley et al.*, 2003]. Accordingly, c is low for optically clear rivers, and high for turbid rivers.

[6] In rivers, the amount of light at depth is ultimately dictated by the diffuse attenuation coefficient (K_d), which depends weakly on features of the light field such as solar zenith angle, the ratio of diffuse to direct solar radiation, and diffuse light within the water column. While K_d is more relevant to primary productivity (via light penetration), c is more relevant to human aesthetics and faunal movements (via visibility). Both variables are important to water resources and aquatic ecology, but we focus here on the inherent optical properties of a, b, and c so that we can use additive principles and compare spatiotemporal trends in OWQ not associated with changes in the solar radiation field. That is we wanted to focus on the rivers' compositional variability in order to parse out the different controls on beam attenuation within the water column (e.g., scattering by particulates versus absorption by dissolved constituents). Further, K_d and c are strongly correlated [*Davies-Colley and Nagels*, 2008] and thus trends in K_d generally follow those of c.

[7] Any component of the water column can absorb and scatter light, but there are only five that significantly attenuate light in rivers: water (w), chromophoric dissolved organic matter (CDOM), inorganic suspended sediment (SS), nonalgal particulate organic matter (POM), and phytoplankton (PHYTO) [*Davies-Colley et al.*, 2003]. Because beam attenuation is an additive process [*Kirk*, 1994], the sum of beam attenuation by each one of these components sets the clarity of a river such that:

$$c = c_w + c_{CDOM} + c_{SS} + c_{POM} + c_{PHYTO} \tag{2}$$

$$c = c_w + c_d + c_p \tag{3}$$

where c_d is the beam attenuation coefficient of the dissolved constituents (c_{CDOM}) and c_p is the beam attenuation coefficient of the particulate constituents ($c_{SS} + c_{POM} + c_{PHYTO}$).

[8] While every river possesses a unique OWQ regime, the spatial and temporal trends of the above five components [*Davies-Colley et al.*, 2003; *Golladay*, 1997; *Reynolds*, 2000; *Sedell and Dahm*, 1990; *Syvitski et al.*, 2000; *Walling and Webb*, 1992; *Wetzel*, 2001] allow for a few generalizations. Temporally, rivers have the greatest clarity during base flow (low Q) and the lowest clarity during and immediately following floods (high Q). Spatially, many headwater streams have high clarity owing to very low CDOM, SS, POM, and PHYTO concentrations. As a river increases in size downstream, and source areas of SS and POM are accessed, the river becomes more turbid and clarity decreases. In the lowest reaches of a river, the main stem channel becomes more hydrologically connected to its floodplain, thereby increasing supply of CDOM to the river. The longer residence time of the lower reaches also allows for a greater abundance of PHYTO. This trend of decreasing clarity along the river continuum (headwaters to mouth) is an underlying tenet of the RCC [*Vannote et al.*, 1980], but to our knowledge has not been empirically verified.

[9] This brief review provides a basic understanding of riverine OWQ, but also highlights the fact that comprehensive quantitative studies of OWQ are rare and that much of our current understanding of light-driven processes in rivers is based on assumed knowledge about spatial and temporal patterns of water constituents. To test some of these prevailing assumptions, we analyze IOPs along the river continuum in two Midwestern rivers (Baraboo River and Wisconsin River, Wisconsin, USA), and compare published synoptic data sets. We also analyze temporal IOPs in a small Midwestern stream (Big Spring Creek, Wisconsin, USA) and a large Southeastern river (Deep River, North Carolina, USA).

3. Study Sites

[10] Four nontidal, freshwater U.S. rivers were selected for our study (Figure 1). We assessed temporal trends in IOPs on two of the rivers: Deep River (DR) and Big Spring Creek (BSC). The dissimilarities between these two rivers allowed us to investigate water clarity over a large range of physical characteristics: from a small, relatively clear stream whose hydrology is driven by groundwater (BSC) to a large, relatively turbid river whose hydrology is predominantly driven by surface runoff (DR). We assessed spatial trends in IOPs on the Wisconsin River (WR) and Baraboo River (BR). The dissimilarity in flow regulation between these two rivers allowed us to investigate water clarity along the

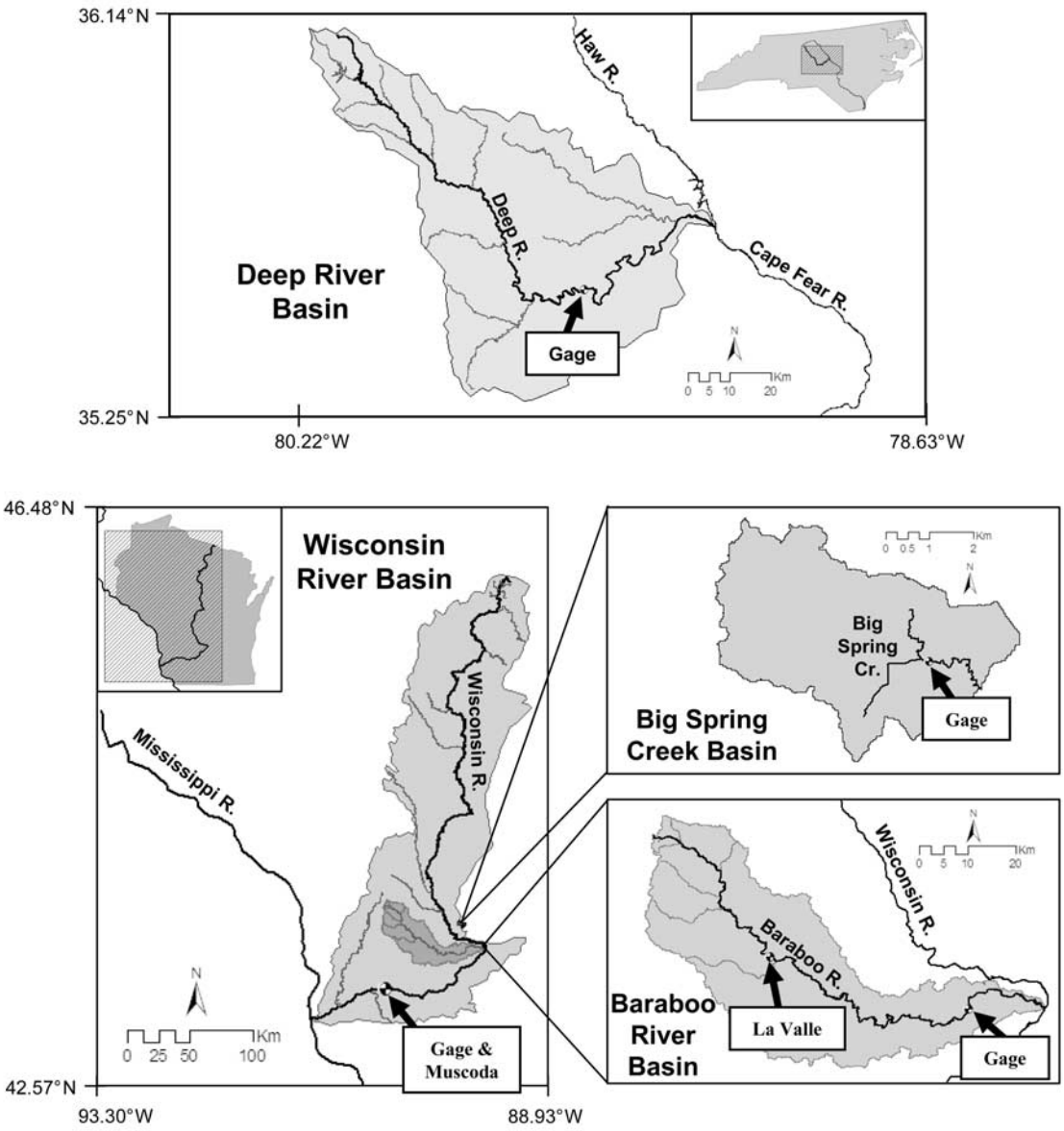

Figure 1. Optical water quality study sites. Major tributaries are depicted for all four basins. Gage identifies where Q was measured and water samples were collected. Big Spring Creek Basin is adjacent to but not located in the Wisconsin River Basin.

river continuum for a heavily regulated river (WR) and an unregulated river (BR).

[11] Deep River is a sixth-order stream located in the Central Piedmont of North Carolina (Figure 1). The 2770-km^2 watershed of the DR gage site is predominantly forest (72%), followed by agriculture (25%) and urban (3%). Its riparian corridor is composed mostly of mixed-hardwood forest. The basin receives 110 cm/a of precipitation with no distinct seasonality (NOAA, National climate data, 2007, available at http://www.noaa.gov/climate.html). Most of the urbanization in the basin is located in the headwaters, which together with its heavily entrenched channels leads to high, flashy flood flows during storms.

[12] Big Spring Creek is a second-order stream located in the Central Plain of Wisconsin (Figure 1). Its 21.1-km^2 drainage basin is mostly agriculture (46%), followed by forest (31%), grassland (21%), and wetland (2%). The riparian corridor of BSC is composed of a mixture of reed canary grass (*Phalaris arundinacea*) and mixed-hardwood forest. Its basin receives 84 cm/a of precipitation with a seasonal peak in monthly precipitation during the summer (see http://www.noaa.gov/climate.html). BSC is a spring-fed stream with relatively constant discharge.

[13] Baraboo River is a sixth-order stream that begins in the Western Uplands of Wisconsin and meanders through the nonglaciated driftless area of central WI before emptying into the Wisconsin River (Figure 1). BR drops in elevation from 420 to 235 m AMSL over a length of 187 km. The 1690-km^2 Baraboo River Basin is mostly agriculture (47%), followed by forest (31%), grassland (15%), wetland (5%), urban (1%), and barren (1%). Its riparian corridor is composed mostly of mixed-hardwood forest and various grasses. BR historically had nine dams on its main stem (see Wisconsin Department of Natural

Table 1. Temporal Sampling of OWQ at Big Spring Creek and Deep River[a]

	21–30 May 2006	14–16 June 2006	11–17 July 2006	29 Aug to 11 Sep 2006	24–26 April 2006	15–24 June 2006	24 June 2005 to 18 Sep 2006
Location	DR	DR	DR	DR	BSC	BSC	BSC
Method	automated	manual	automated	automated	automated	automated	manual
Flow	base flow	flood	base flow	flood	base flow	base flow	base flow/flood[b]
Sample interval (hours)	12	~24	6	6	4	6	discrete
Sample number	20	3	25	50	12	36	22/2

[a]Automated samples were collected with Teledyne-ISCO 6712 autosamplers. Manual samples were collected following the protocol in section 4.1. All samples were kept dark and refrigerated at ~4°C, and analyzed within 72 hours of sample collection, with only two exceptions (two flood samples for BSC). Abbreviations are as follows: DR, Deep River; BSC, Big Spring Creek.

[b]The two flood samples for BSC were collected at a station ~2 km downstream of the study site. A paired *t*-test (n = 44) revealed that *c* was not statistically different between these two sites ($t = -1.36$, p = 0.18).

Resources' Dam Database; available at http://dnr.wi.gov/org/water/wm/dsfm/dams/datacentral.html; hereinafter referred to as WDNR, 2006). All nine dams have been removed, the last one in 2001, and now its entire 187-km main stem is free-flowing.

[14] Wisconsin River is a seventh-order stream that begins at Lac Vieux Desert in the Northern Highlands of Wisconsin and empties into the Mississippi River (Figure 1). It drops in elevation from 515 to 185 m AMSL over a length of 684 km. The 31,400-km^2 Wisconsin River Basin is mostly forest (41%), followed by agriculture (27%), wetland (15%), grassland (11%), open water (3%), urban (1%), shrubland (1%), and barren (1%). Its riparian corridor is composed of a mosaic of wetlands, prairie, oak savanna, and floodplain forest. There are currently 26 main stem dams on the Wisconsin River (WDNR, 2006).

4. Methods

4.1. Sample Collection

[15] We compared short-term (3–10 d) and long-term (April-September) changes in OWQ during base flow and flood conditions at DR and BSC to assess temporal trends (Table 1). We assessed longitudinal trends in OWQ by performing synoptic surveys along the continuum of BR and WR. Water samples were collected during base flow from 23 main stem locations and 7 tributaries along BR on 13 August 2006 and from 20 main stem locations along WR on 16 September 2006. All samples were collected in acid-washed amber polyethylene bottles except DOC samples, which were collected in precombusted glass vials treated with 600 μL of 2M HCl. All filtered water samples, including DOC, were obtained using *Whatman* GF/F (0.7 μm) glass fiber filters [*Wetzel and Likens*, 2000]. Water chemistry and OWQ analyses were performed within 72 h of sample collection. All water samples were kept dark and refrigerated at ~4°C until analysis, which minimized any changes in water chemistry during this time.

4.2. Hydrology

[16] We obtained 15-min discharge records from the USGS gages #05405000 and #05407000 for BR and WR, respectively. Discharge records for BSC and DR were obtained from stage-*Q* rating curves we developed using 15-min water-level readings from stage recorders (*Intech WT-HR 2000* for BSC and *HOBO 9-m* for DR) and in situ *Q* measurements taken with a *Marsh-McBirney* current meter.

4.3. Water Chemistry

[17] We measured total suspended solids (TSS) and its fractionated components of SS and POM on all water samples according to APHA Standard Methods procedure 2540D/E [*Clesceri et al.*, 1998] using 1.5 μm glass fiber filters (*ProWeigh, Environmental Express*). We measured DOC as nonpurgeable organic carbon (NPOC) with a *Shimadzu* TOC-Vcsh Analyzer according to APHA Standard Methods procedure 5310B [*Clesceri et al.*, 1998]. We used *chl-a* concentration as a proxy for PHYTO concentration. For DR, BSC, and BR, we measured *chl-a* with a *Turner Designs* TD-700 fluorometer according to APHA Standard Methods procedure 10200H [*Clesceri et al.*, 1998] using *Whatman* GF/F glass fiber filters. For WR, we measured *chl-a* with a *Beckman DU Series 600* UV/VIS spectrophotometer according to *Hauer and Lamberti* [1996].

4.4. Optical Measurements

4.4.1. Turbidity (T_n)

[18] We measured T_n with a *Hach* 2100P turbidimeter in nephelometric turbidity units (NTU), which is a relative measure of *b* [*Kirk*, 1994]. We used the average value of three T_n measurements for each sample, thoroughly mixing the sample prior to each measurement.

4.4.2. Inherent Optical Properties

[19] We used a *Beckman DU Series 600* UV/VIS spectrophotometer to determine the IOPs of water samples. The spectrophotometer measured the amount of incident radiant flux (Φ_0) that was received by a light detector (Φ) after being transmitted through a water sample path length (*r*). All water samples were contained in the same quartz cuvette ($r = 0.01$ m) and analyzed at room temperature (21°C). Adopting the method of *Bricaud et al.* [1983], we derived the beam attenuation coefficient (*c*) with a *Beckman* turbidity cell holder (TCH), which prevented scattered light from reaching the light detector by reducing the collection angle to 0.94° (collimated light beam) and moving the water sample to 52 mm from the light detector. With this configuration, the light detector only captured the incident light that was left after absorption and scattering by the water sample. Using the TCH, *c* was calculated as follows:

$$c = -\ln(\Phi/\Phi_0)_{\mathrm{TCH}}/r \quad (4)$$

We derived the absorption coefficient (*a*) by using a *Beckman* standard cell holder (SCH), which placed the

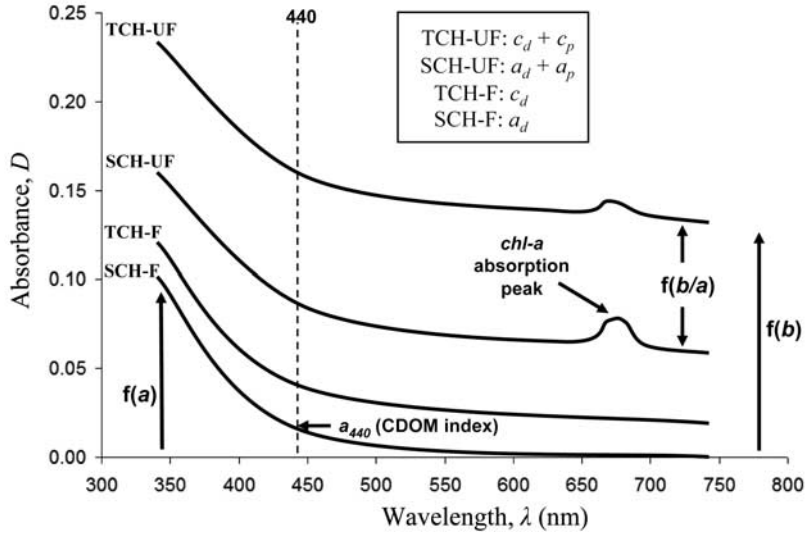

Figure 2. Heuristic diagram of the four-configuration spectrophotometer scan. The magnitude of absorbance at 740 nm illustrates the degree of scattering. The magnitude of absorbance at 440 nm of filtered water samples illustrates the absorption by CDOM. The proportional spacing between the top two absorbance curves illustrates the scattering to absorption ratio (*b/a*). The relative height of the peak in the SCH-UF absorbance curve at 675 nm indicates the magnitude of light attenuation by phytoplankton.

water sample 10 mm from the light detector and increased the collection angle to 14°. At this close proximity and comparatively large collection angle we expect, on the basis of published volume scattering functions [*Petzold*, 1972], most (~75%) of the scattered light to be detected, thus absorption can be quantified once a correction for undetected scattered light is applied. Residual scattering not captured by the light detector was corrected for by subtracting out the apparent absorption coefficient at 740 nm (X_{740}) because essentially all measured absorption at 740 nm is due to scattering [*Davies-Colley et al.*, 2003]. Using the SCH, a was calculated as follows:

$$X = -\ln(\Phi/\Phi_0)_{\mathrm{SCH}}/r \tag{5}$$

$$a = X - X_{740} \tag{6}$$

where X is the apparent absorption coefficient for the measured wavelength. Equation (6) assumes that angular distribution of scattering is spectrally independent, and that the spectral trend of scattering is negligible. Using equation (1), we calculated the scattering coefficient (b) by subtracting a from c, as recommended by *Davies-Colley et al.* [2003].

4.4.3. Spectrophotometer Scans

[20] We scanned each water sample in 1-nm intervals between 340 and 740 nm at 1200 nm/min. Each scan took approximately 20 s, thus we assumed that particulate settling was minimal. Each sample was thoroughly mixed prior to each scan. In order to derive the variables in equations (4)–(6) and partition c (described below), we performed four configurations of scans on each water sample (Figure 2): TCH-UF (turbidity cell holder, unfiltered sample), TCH-F (turbidity cell holder, filtered sample), SCH-UF (standard cell holder, unfiltered sample), SCH-F (standard cell holder, filtered sample). We performed 3 scans for each configuration and used mean values for subsequent analyses. From the spectrophotometer scans, we used readings at 440 nm (index of CDOM), 740 nm (residual scattering), and the average of 400–700 nm (PAR). Unless denoted by a subscript identifier (e.g., a_{440}), all reported attenuation coefficients are average values for PAR.

[21] We also used the spectrophotometer scans to compare IOPs between the four study sites and to previous studies. The spectrophotometer scans (Figure 2) illustrate the change in absorbance (D) with wavelength (λ), where:

$$D = \log_{10}(\Phi_0/\Phi) \tag{7}$$

The magnitude of absorbance at 740 nm illustrates the degree of scattering in the water column, which indicates the concentration of particulates since scattering by dissolved constituents is negligible. The magnitude of absorbance at 440 nm of filtered water samples illustrates the absorption by CDOM. The proportional spacing between the top two absorbance curves (TCH-UF and SCH-UF) illustrates the scattering to absorption ratio (*b/a*), which indicates the dominant process of beam attenuation. The magnitude of beam attenuation by PHYTO is indicated by the relative height of the peak in the SCH-UF absorbance curve at 675 nm [*Gallegos and Neale*, 2002], which is an absorption peak of *chl-a*.

4.5. Partitioning Light Beam Attenuation

[22] We partitioned the beam attenuation coefficient into its constituent fractions (equation (3)) by using combinations of TCH versus SCH and UF versus F (Figure 3). Using the TCH on an unfiltered sample quantifies the collective beam attenuation coefficient by the dissolved (c_d) and particulate (c_p) constituents. Because the spectrophotometer was blanked with Milli-Q water prior to measurements, we added the beam attenuation coefficient of pure water (c_w) to the TCH-UF reading to obtain the total beam attenuation coefficient (c). Values for c_w, a_w, and b_w were

	Turbidity Cell Holder (TCH)		Standard Cell Holder (SCH)		(TCH – SCH)
Unfiltered Sample (UF)	c	=	a	+	b
	=		=		=
Filtered Sample (F)	c_d	=	a_d	+	b_d
	+		+		+
(UF – F)	c_p	=	a_p	+	b_p
	+		+		+
Pure Water	c_w	=	a_w	+	b_w

Figure 3. Partitioning of the beam attenuation coefficient using the four-configuration spectrophotometer scan.

obtained from the data of *Buiteveld et al.* [1994]. Using the SCH on an unfiltered sample quantifies the collective light absorption coefficient by the dissolved (a_d) and particulate (a_p) constituents. We added the absorption coefficient of pure water (a_w) to the SCH-UF reading to obtain the total light absorption coefficient (a). Using the TCH on a filtered sample quantifies c_d. Using the SCH on a filtered sample quantifies a_d. We derived particulate attenuation coefficients by subtracting the dissolved and water attenuation coefficients from the total attenuation coefficients (equation (3)). For example, $c_p = c - c_d - c_w$ (TCH-UF – TCH-F; Figure 3). We derived scattering coefficients by subtracting the absorption coefficients from the beam attenuation coefficients (equation (1)).

[23] We partitioned c_p into c_{SS} and c_{POM} by using the a_p and b_p of water samples where TSS was 100% POM. When the particulates in a water sample are composed entirely of POM, b_p can be attributed entirely to POM ($b_p = b_{POM}$). Because absorption by SS is usually negligible (*Davies-Colley et al.* [2003]; exceptions include iron oxides: *Babin and Stramski* [2004]), a_p for any water sample can be attributed entirely to POM ($a_p = a_{POM}$). If we define K as b_{POM}/a_{POM}, then under this scenario $b_{POM} = \mathrm{K}a_p$, which allows us to approximate the beam attenuation coefficient of POM:

$$c_{POM} = a_{POM} + b_{POM} = a_p + \mathrm{K}a_p \tag{8}$$

This equation assumes that K is a constant for all POM in the water column. It also assumes that c_{PHYTO} is negligible or either incorporated into c_{POM}.

4.6. Water Clarity Budget

[24] We quantified the effect of tributaries on spatial OWQ trends by creating a water clarity budget for the Baraboo River using the mass balance approach of *Davies-Colley et al.* [2003]:

$$c_{ds}Q_{ds} = c_{us}Q_{us} + c_{trib}Q_{trib} \tag{9}$$

where c is the beam attenuation coefficient in m^{-1}, Q is discharge in m^3/s, and the subscripts *ds*, *us*, and *trib* denote downstream, upstream, and tributary, respectively. This method assumes that c is volume conservative, where constituents do not experience physical or chemical changes (e.g., sedimentation of SS) between the upstream and downstream sites. To obtain c, we used equation (4) on water samples collected from seven confluences. At each confluence, we sampled immediately upstream of the confluence (c_{us}), at the tributary outlet before it entered the main stem channel (c_{trib}), and below the confluence at a sufficient distance downstream to allow full mixing but upstream of the next downstream confluences (c_{ds}). Q was derived with the weighted area method [*Gordon et al.*, 2004], using the downstream USGS gage at river kilometer (RK) 160. Watershed areas were calculated with the ArcHydro extension in ArcGIS 9.1 (*ESRI*). We used high-resolution (1:24,000) national hydrography data (USGS) to characterize stream-link magnitudes (i.e., stream order via the Strahler method) [*Gordon et al.*, 2004]. "Major" tributaries (in the sense of *Benda et al.* [2004]) were identified on the basis of a stream order greater than or equal to n − 1, where n is the stream order of the main stem channel before the confluence.

4.7. Synoptic Optical Water Quality Data Sets

[25] We assessed global longitudinal trends in OWQ by comparing our two longitudinal c profiles from BR and WR with published synoptic data sets that met two conditions: (1) OWQ was measured in at least five locations from near

Table 2. Discharge and Water Chemistry of Gage Sites[a]

	Deep River at Glendon[b]	Big Spring Creek at Big Spring[b]	Baraboo River at La Valle[b,c]	Wisconsin River at Muscoda[d]
Q (m^3/s)	9.7 ± 14.4	0.29 ± 0.02	9.6 ± 6.0	193.1 ± 77.7
DOC (mg/L)	6.8 ± 1.4 (65)	1.2 ± 0.3 (94)	2.7 ± 0.2 (43)	6.9 ± 0.6 (8)
SS (mg/L)	20.1 ± 55.9 (124)	4.3 ± 3.0 (64)	60.7 ± 24.3 (50)	28.1 ± 39.2 (32)
POM (mg/L)	5.2 ± 8.4 (124)	2.5 ± 1.0 (64)	8.9 ± 2.3 (50)	16.6 ± 5.1 (32)
chl-a (μg/L)	1.5 ± 1.1 (21)	6.3 ± 1.0 (10)	28.0 ± 11.3 (10)	45.4 ± 23.3 (7)

[a]Values are mean ± standard deviation (number of observations). Q data for all four sites is from water year 2006.
[b]From this study.
[c]Q from USGS gage 05405000.
[d]From *Popp* [2005] and USGS gage 05407000.

the headwaters to the river's mouth; and (2) the main stem channel was greater than 100 km. Three data sets fulfilled these criteria, all from New Zealand: Motueka River (110 km; *Davies-Colley* [1990]), Pomahaka River (147 km; *Harding et al.* [1999]), and Waikato River (330 km; *Davies-Colley* [1987]). The Waikato River study reported Secchi disk depth (z_{SD}), which we converted to c using the method of *Gordon and Wouters* [1978] ($c = 6/z_{SD}$). The Pomahaka and Motueka River studies reported black disk visibility (y_{BD}), which we converted to c using the method of *Davies-Colley* [1988] ($c = 4.8/y_{BD}$). We used these five synoptic OWQ surveys to test the prediction of the RCC [*Vannote et al.*, 1980] that water clarity decreases along the river continuum from headwaters to mouth.

5. Results

5.1. Optical Water Quality Comparisons

[26] Big Spring Creek (BSC) had the highest clarity because of its low SS, POM, DOC, and PHYTO (Table 2). These characteristics caused the water of BSC to be relatively colorless owing to the lack of scattering or absorption of light. BSC had the lowest average base flow c at 2.73 ± 0.89 m^{-1} (mean±std. dev.) and the lowest average base flow T_n at 4.0 ± 1.3 NTU of the four study sites (Table 3). Deep River (DR) had a yellowish hue owing to preferential blue-light absorption by its high DOC concentration. The average base flow c and T_n for DR was 5.78 ± 1.57 m^{-1} and 5.0 ± 1.9 NTU, respectively. Wisconsin River (WR) at Muscoda also had a yellowish hue due its high DOC concentration. The c and T_n for WR at Muscoda were 15.71 m^{-1} and 13.6 NTU. Baraboo River (BR) at La Valle had the lowest clarity predominantly because of high SS and POM which imparted a dark-brownish hue on the water. This site had the highest c and T_n of the four study sites at 29.26 m^{-1} and 27.4 NTU.

[27] Spectrophotometer scans of base flow samples illustrated the relative differences in IOPs among the four study sites (Figure 4). BR had the highest TCH-UF absorbance curve at 740 nm and thus had the highest total scattering coefficient (b) at 25.41 m^{-1}, followed by WR at 13.13, DR at 4.39, and BSC at 2.53. We found a strong correlation between TSS (SS + POM; Table 2) and b ($r^2 = 0.98$, $p = 0.027$), which supports the expected increased scattering with increased concentration of particulates. DR had the highest SCH-F absorbance curve at 340 nm and thus had the highest CDOM absorption coefficient (a_{440}) at 4.44 m^{-1}, followed by WR at 2.36, BR at 1.60, and BSC at 0.41. DOC explained 82% of the variation in a_{440}, although the regression was not statistically significant ($p = 0.135$), likely owing to the small sample size (n = 4).

[28] At all four sites, scattering was the dominant process of beam attenuation ($b/a > 1$), with BR having the highest b/a at 6.60, followed by WR at 5.08, BSC at 4.10, and DR at 1.64. The magnitude of beam attenuation by PHYTO was negligible at DR and BSC because of the lack of a peak at 675 nm in the SCH-UF absorbance curves (Figure 4). Their low *chl-a* concentrations (Table 2) support this result. BR and WR had small peaks at 675 nm owing to higher *chl-a*, which still contributed minimally to overall beam attenuation.

[29] Turbidity was a highly significant ($p < 0.001$) predictor of c at all four sites (Figure 5). The regression slopes of ~1 for BR and WR, which represent longitudinal changes in c versus T_n throughout the basin, agree well with other studies that measured both variables across space [*Davies-Colley*, 1987; *Davies-Colley and Smith*, 1992]. The much lower regression slopes for DR and BSC, which represent changes in c versus T_n with varying discharge at a station, was likely due to the ratio of 90° scattering to total scattering (T_n/b) being lower for the larger particles suspended by more energetic flows [*Davies-Colley and Close*, 1990].

Table 3. Base Flow Turbidity and IOPs of Study Sites[a]

	Deep River at Glendon	Big Spring Creek at Big Spring	Baraboo River at La Valle	Wisconsin River at Muscoda
T_n (NTU)	5.0 ± 1.9	4.0 ± 1.3	27.4	13.6
c (m^{-1})	5.78 ± 1.57	2.73 ± 0.89	29.26	15.71
b/a	1.25 ± 0.29	2.63 ± 0.87	6.60	5.08
a_{440} (m^{-1})	4.10 ± 1.09	0.61 ± 0.20	1.60	2.36

[a]Study sites are: Deep River (n = 74), Big Spring Creek (n = 49), Baraboo River (n = 1), and Wisconsin River (n = 1). Values are mean ± standard deviation.

5.2. Temporal Trends: Deep River and Big Spring Creek

5.2.1. Turbidity and Discharge

[30] Turbidity generally increased with increasing Q for DR and BSC (Figure 6). Q explained 77% of the variation in T_n at DR (Figure 6b; $p < 0.001$). We attribute this unexplained variation to hysteresis, interstorm, and seasonal effects. For example, T_n values for the storm on 14 June 2006 were lower, despite being a larger flood, than the

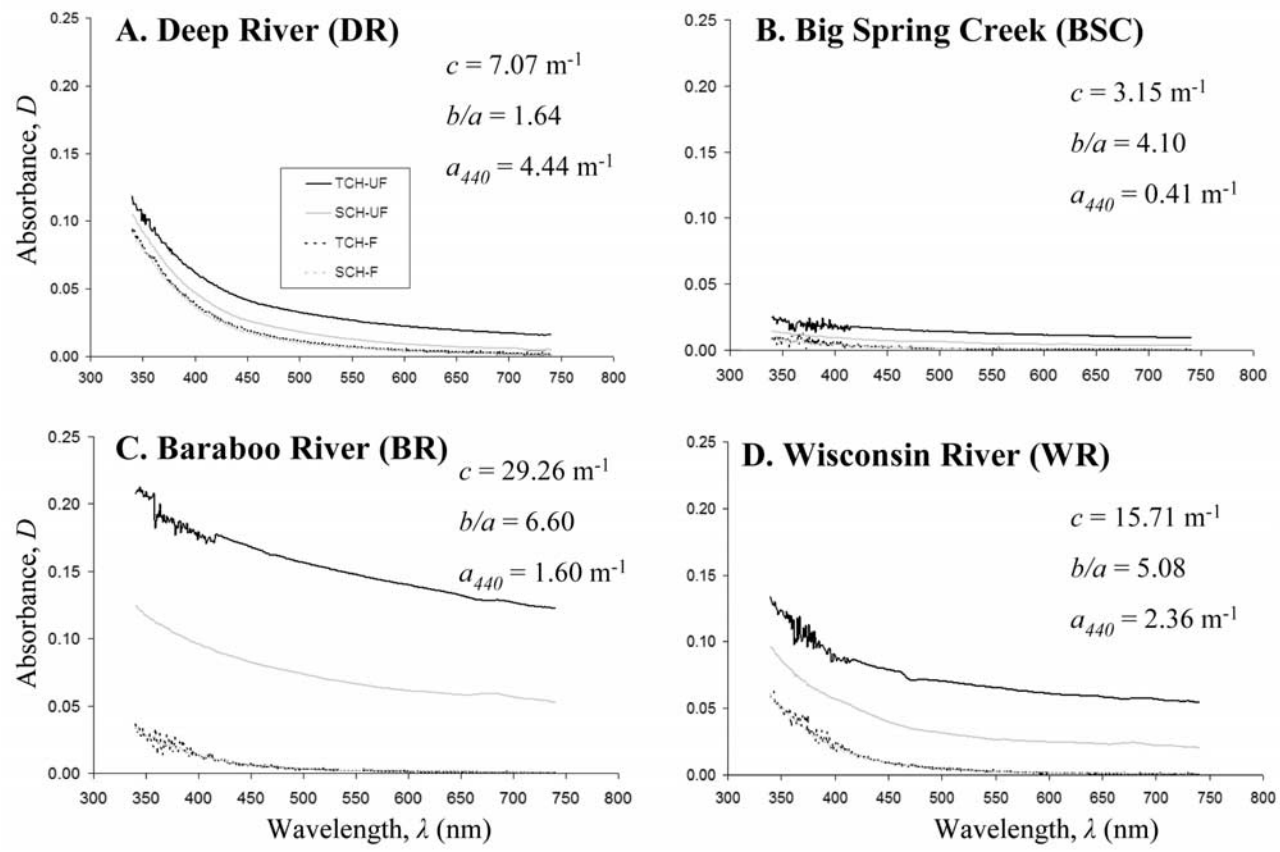

Figure 4. Representative spectrophotometer scans of the four study sites during base flow.

storm on 30 August 2006 (Figure 6a). The two likely causes for this scenario are: (1) There was a separate flood on 13 June 2006 that depleted the accumulated source of fine sediment and POM for the 14 June flood, and/or (2) More sediment and POM were available for the 30 August storm owing to crop harvesting during this time. The relationship between c and Q at DR (r^2 = 0.71; $c = 1.43Q^{1.04}$) was similar to the relationship between T_n and Q.

[31] Discharge explained only 27% of the variation in T_n at BSC (Figure 6d; $p < 0.001$). We attribute most of this unexplained variation to seasonal effects. The reduced vegetative ground coverage of BSC basin during the winter allowed greater surface sediment runoff, especially during the numerous snowmelt runoff events that occurred in central Wisconsin during the 2005–2006 winter. This scenario is the likely cause of the two high T_n measurements in March 2006 (Figure 6c). The other considerable seasonal effect on T_n in BSC was the die-off of in-channel vegetation during late summer. BSC had a dense benthic coverage of aquatic macrophytes, which began to senesce in late July [*Zahn*, 2007]. This senescence not only added plant fragments to the water column, but also fine sediment that was previously trapped by the vegetation. This scenario is the likely cause of the increasing T_n values starting in August of both years. Another contributing factor to increased T_n at BSC was observed bioturbation, with the greatest turbidity pulses being caused by cows and geese. The extremely high T_n in February 2006 (64 NTU) was most likely caused by one of these two animals. The relationship between c and Q at BSC (r^2 = 0.43; $c = 1370.9Q^{4.85}$) was similar to the relationship between T_n and Q.

5.2.2. Base Flow Beam Attenuation of Big Spring Creek

[32] The clarity of Big Spring Creek varied relatively little during the 10-d base flow period from 15 to 24 June 2006 (Figure 7a). Particulates (c_p: 81%) accounted for most of the beam attenuation, followed by CDOM (c_d: 13%) and water (c_w: 6%). The particulates consisted of 47% POM (2.2 mg/L) and 53% mineral sediment (2.7 mg/L). The concentration of *chl-a* was relatively low and constant over the 10 d (6.3 ± 1.0 μg/L). The base flow period of BSC was characterized by small and brief pulses of SS, POM, and CDOM. Overall, CDOM (a_{440}) remained fairly constant at 0.67 m^{-1} and TSS decreased from 5.4 to 3.4 mg/L. The decrease in TSS was therefore the cause for the decrease in c over the 10-d period, from 3.3 to 2.0 m^{-1}.

5.2.3. Base Flow Beam Attenuation of Deep River

[33] The clarity of Deep River increased slightly during the 10-d base flow period from 21–30 May 2006 (Figure 7b). During this base flow period, c_p accounted for most (64%) of the beam attenuation, followed by c_d (33%) and c_w (3%). The particulates consisted of 34% POM (2.1 mg/L) and 66% mineral sediment (4.1 mg/L). The concentration of *chl-a* was minimal and relatively constant over the 10 d (1.2 ± 0.1 μg/L). The base flow period of DR was characterized by decreases in SS (5.6 to 2.9 mg/L) and CDOM (4.4 to 2.2 m^{-1}), resulting in a decrease of c from 6.7 to 3.6 m^{-1}. During this time, POM % increased at an average rate of 3.0% per day (20 to 50%). TSS, however,

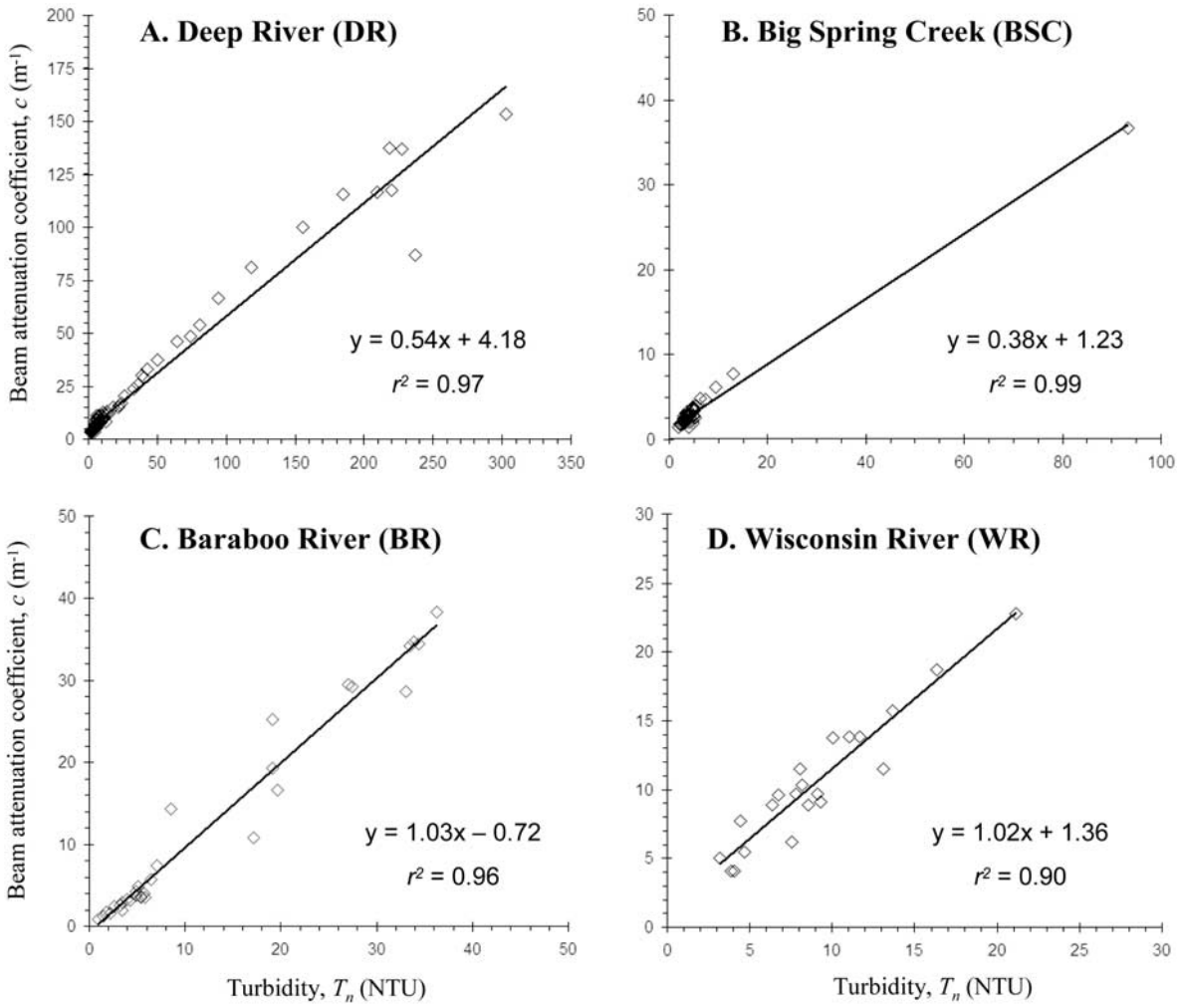

Figure 5. Beam attenuation coefficient (c) versus turbidity (T_n) for the four study sites. DR and BSC illustrate changes in c versus T_n in response to changes in Q at a station. BR and WR illustrate longitudinal changes in c versus T_n throughout the basin. Note the different x- and y-axes between the plots.

remained fairly constant at 6.3 mg/L, suggesting that sediment was settling out while additional sources of POM were being added to the water column. During the other base flow sampling period (11–17 July 2006; data not illustrated), POM % increased at an average rate of 4.5% per day (20 to 47%) while TSS remained fairly constant at 7.6 mg/L.

5.2.4. Flood Beam Attenuation of Deep River

[34] In contrast to the limited change in clarity during base flow, the magnitude and composition of c varied greatly through a flood at DR on 30 August 2006 (Figure 7c; Q_{peak} = 60 m^3/s, recurrence interval of ~2 months). This flood occurred following a prolonged (~1 month) low-flow period (Figure 6a) and thus preflood water column concentrations of TSS (3.0 mg/L) and CDOM (2.7 m^{-1}) were relatively low. Before the flood, c was 3.5 m^{-1}, with c_p accounting for most beam attenuation (60%), followed by c_d (35%) and c_w (5%). Preflood POM averaged 87% of TSS. The value of c increased rapidly during the rising limb of the flood due mostly to a pulse of TSS, and c reached a maximum of 137.3 m^{-1} at 12 h after Q_{peak}. This lag was most likely caused by either a delayed sediment peak resulting from the flood wave's celerity being faster than the water velocity or an additional TSS pulse from a tributary with a slower travel time. As particulates settled out of the water column following Q_{peak}, c decreased exponentially until it reached its average base flow value of 5.8 m^{-1} at 8 d following Q_{peak}. CDOM also increased in response to the flood and maintained elevated concentrations during the entire sampling period, which is characteristic of terrestrial subsurface flow following a dry period [*Walling and Webb*, 1992]. Consequently, the relative proportion of beam attenuation by CDOM increased following the flood, reaching a maximum of 53%.

5.2.5. Components of Beam Attenuation

[35] Partitioning the total beam attenuation coefficient (c) by means of equation (3) and Figure 3 revealed that scattering by particulates (b_p) was the dominant process of midsummer base flow beam attenuation at DR and BSC (Table 4). Absorption by CDOM (a_d) and particulates (a_p) were the two other main contributors to base flow beam attenuation at both sites. For all combined base flow

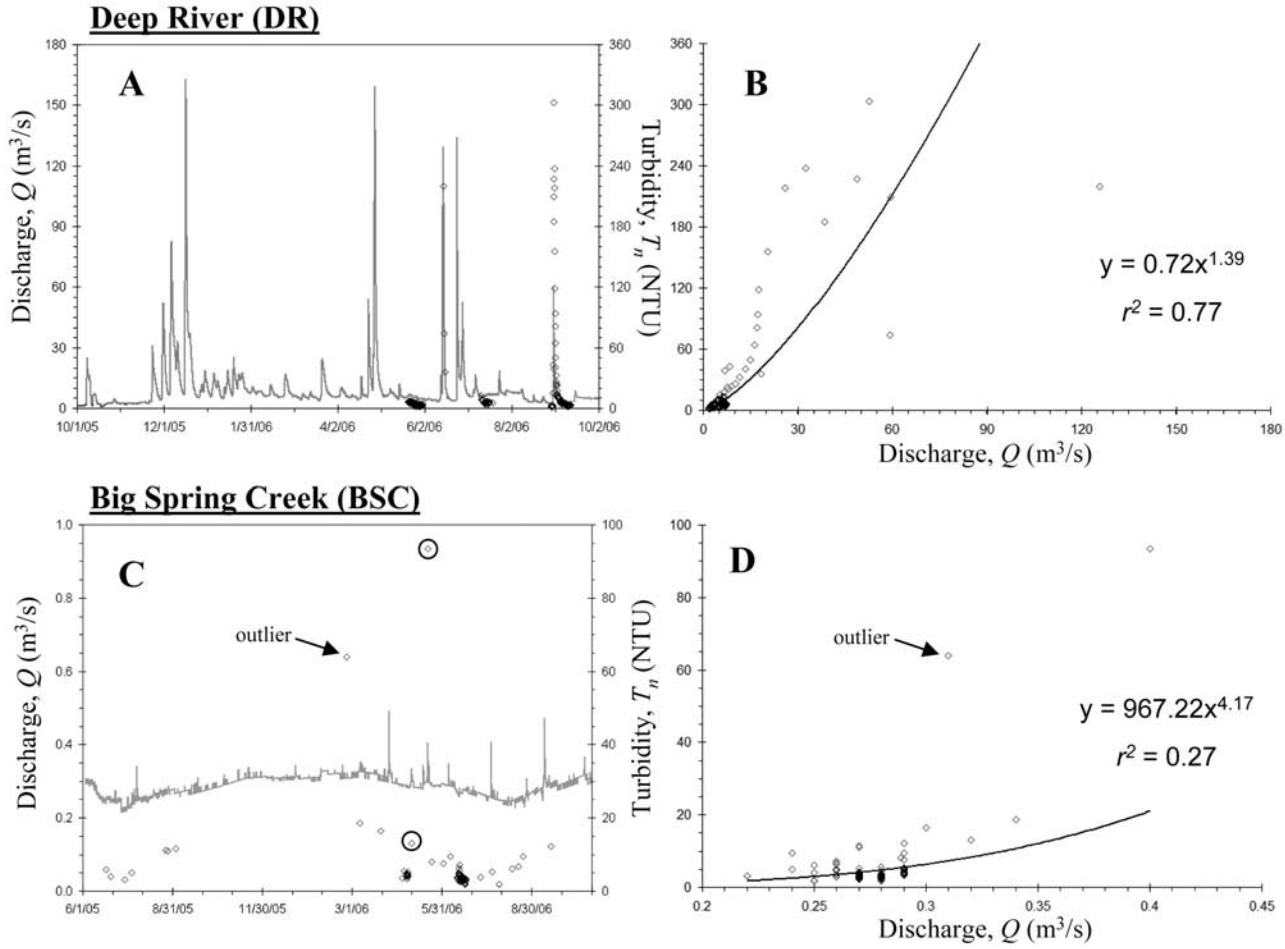

Figure 6. Discharge (Q, time series) and turbidity (T_n, point samples) for (a and b) Deep River and (c and d) Big Spring Creek. The four tightly grouped sample intervals in Figure 5a are the four sampling periods for DR. The two tightly grouped sample intervals in Figure 5c are the two sampling periods for BSC. Circled values in Figure 5c are the two flood samples of BSC. The outlier (from bioturbation) was not factored into the regression analysis in Figure 5d. Note the different x- and y-axes between DR and BSC.

sampling at BSC, c averaged 2.73 ± 0.89 m^{-1}, of which 82% was from TSS (c_p), 12% from CDOM (c_d), and 6% from water (c_w). For all combined base flow sampling at DR, c averaged 5.78 ± 1.57 m^{-1}, of which 60% was from TSS (c_p), 37% from CDOM (c_d), and 3% from water (c_w).

[36] Using water samples where TSS was virtually 100% POM, we found that b_{POM}/a_{POM} (or K; see Section 4.5.) for DR was ~3 (3.06 ± 0.65, n = 5). There were no water samples from BSC where TSS was 100% POM, and therefore we used K from DR for BSC. This assumes that POM composition is similar between DR and BSC, which is reasonable on the basis of their riparian zones both being composed of mixed-hardwood forest. Assuming that K equals 3, the beam attenuation coefficient of POM (c_{POM}) is approximately $4a_p$ (equation (8)). Using equation (8) and Table 4, we calculated the amount of base flow beam attenuation by water, CDOM, SS, and POM at each site (Figure 8). Beam attenuation by PHYTO was included in POM, but given its low concentrations at both sites (Table 2), its contribution to beam attenuation was probably minimal. *Vahatalo et al.* [2005] found that a_{PHYTO} for the Neuse River basin, which is adjacent to the Deep River basin and had slightly higher *chl-a* concentrations than DR, contributed 2.3 ± 2.9 % to a. During base flow at DR, POM (43%) was the greatest contributor to beam attenuation, followed by CDOM (37%), SS (17%), and water (3%). During base flow at BSC, POM and SS both contributed 41% to total beam attenuation, followed by CDOM (12%) and water (6%).

5.3. Spatial Trends: Baraboo River and Wisconsin River

5.3.1. Wisconsin River Continuum

[37] Particulate and dissolved concentrations in the water column fluctuated greatly along the 684-km WR for the first 550 km, with sporadic increases and decreases in all four components (Figure 9a). The large fluctuations in water chemistry were likely associated with major tributary inputs and impoundments along this section of river (Figure 9b). Downstream of the last main stem dam (RK 538), SS, POM, and PHYTO steadily increased, while CDOM remained fairly constant. SS, POM, and PHYTO all reached their maximum values at the last sampling site (RK 674). The scattering to absorption ratio (b/a) along WR was highly

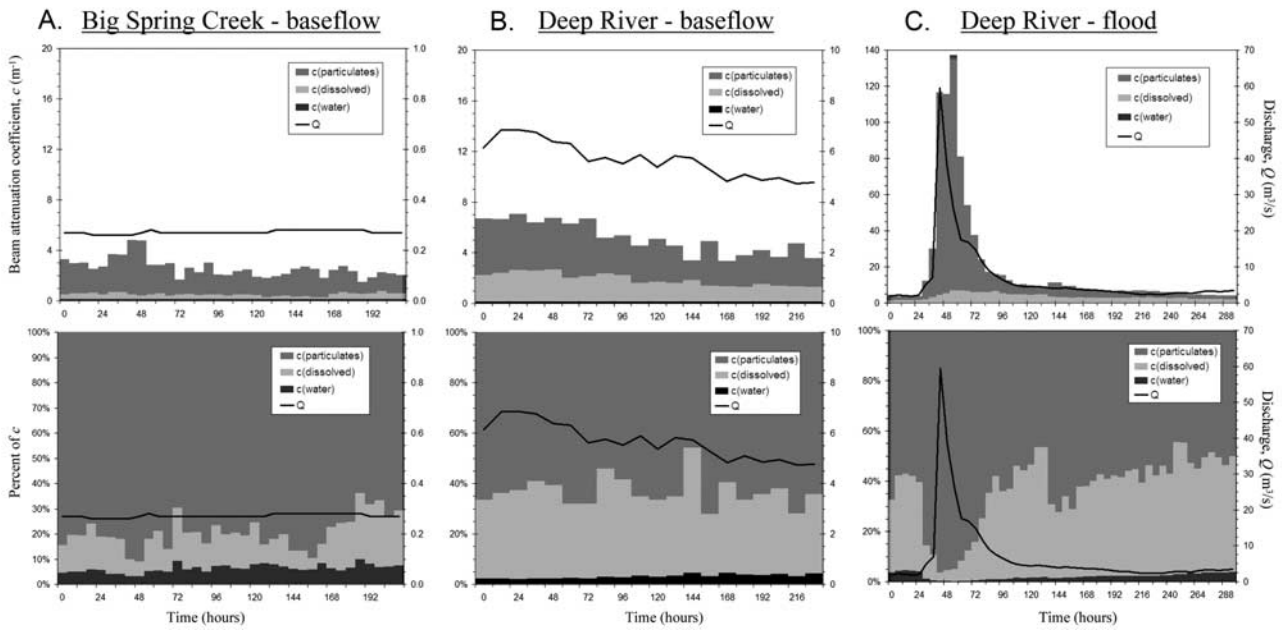

Figure 7. Partitioned beam attenuation at (a) Big Spring Creek during base flow (15–24 June 2006), (b) Deep River during base flow (21–30 May 2006), and (c) Deep River during a flood (29 August to 11 September 2006). Note the different y-axes between base flow and flood.

irregular, ranging from 1.8 (RK 205) to 5.3 (RK 674), indicating large changes in SS and POM relative to CDOM.

[38] The beam attenuation coefficient (c) along WR followed a similar trend as SS and POM by fluctuating between 4.1 and 13.8 m^{-1} for the first 548 km and then steadily increasing after the last main stem dam, reaching a maximum of 22.8 m^{-1} (Figure 9b). There were two local peaks in c along WR, both of which occurred immediately downstream of confluences with turbid major tributaries. Between RK 250 and 292 (Big Rib River confluence at RK 256), c increased from 8.9 to 13.8 m^{-1}. Between RK 488 and 524 (Baraboo River confluence at RK 506), c also increased from 8.9 to 13.8 m^{-1}. The c of BR before it entered WR was 25.2 m^{-1} (Figure 10b).

5.3.2. Baraboo River Continuum

[39] Water chemistry along the 187-km BR (Figure 10a) fluctuated less than along WR. CDOM remained fairly constant along the entire length of BR. SS and POM increased slightly over the first 28 km, and then rapidly over the next 46 km. After RK 74, SS decreased gradually and POM decreased rapidly. The increase in SS and POM at RK 28 was immediately downstream of the confluence of a turbid major tributary (Cleaver Creek, RK 25). PHYTO along BR was not measured directly, and therefore we relied on the relative peak height at 675 nm in the SCH-UF absorbance curve (Figure 2) to make inferences on its longitudinal distribution. PHYTO was minimal in the headwaters (i.e., no peak), increased gradually to RK 40, and then decreased gradually toward the mouth of BR. This decrease in PHYTO at RK 40 coincided with a sharp increase in c (Figure 10b), indicating less favorable conditions for their growth. The scattering to absorption ratio (b/a) increased along BR from 0.8 (RK 3) to 7.8 (RK 142), before decreasing to 5.9 at the mouth (RK 181). The increase in b/a was associated with increased concentrations of SS and POM while CDOM remained relatively constant. The decrease in b/a over the last 39 km of BR was associated with decreased concentrations of SS and POM (Figure 10a) and lower channel gradient (Figure 10b), which indicates that the particulates were likely settling out of the water column over this reach.

[40] The trend of c along BR was similar to that of SS and POM: (1) increasing gradually over the first 38 km; (2) increasing rapidly over the next 34 km; (3) increasing gradually over the next 70 km; and (4) decreasing rapidly over the last 39 km (Figure 10b). These trends in c matched the pattern of major confluences along BR, where c increased rapidly after three major confluences and began to decrease 40 km downstream of the last major confluence.

5.4. Water Clarity Budget of Baraboo River

[41] We used the synoptic c and Q data through the BR watershed to develop a water clarity budget (Figure 11) in which we quantified the relative influence of tributary clarity (c_{trib}) on main stem clarity (c_{us}; equation (9)). All but two of the tributaries sampled were major tributaries (Kratche Creek and Narrows Creek) and two of the major tributaries from Figure 10b were not sampled (Cleaver Creek at RK 25 and Seymour Creek at RK 34). Generally, c_{trib} and Q_{trib} increased in the downstream direction. The value of c_{us} increased in the downstream direction for the first 73 km, but then leveled off or decreased. The rate of increase in c_{us} (0.38 m^{-1}/km) over the first 73 km was more than two times the rate of increase in c_{trib} (0.17 m^{-1}/km), which resulted in a clarity inversion in which c_{trib} was greater than c_{us} in the upper basin, but lower than the c_{us} in lower basin. Accordingly, the largest increase in c (+3.22 m^{-1}) occurred in the upper basin at the West Branch Baraboo River confluence, while the largest decrease in c (−4.82 m^{-1}) occurred in the lower basin at the Narrows Cr. confluence.

Table 4. Partitioned Base Flow IOPs for Deep River and Big Spring Creek[a]

	c	c_w	c_d	c_p	a	a_w	a_d	a_p	b	b_w	b_d	b_p
DR	5.78 ± 1.57 (100)	0.15 (3)	2.15 ± 0.64 (37)	3.48 ± 1.13 (60)	2.57 ± 0.67 (45)	0.15 (3)	1.80 ± 0.49 (31)	0.63 ± 0.25 (11)	3.20 ± 1.03 (55)	0.00 (0)	0.35 ± 0.20 (6)	2.85 ± 0.95 (49)
BSC	2.73 ± 0.89 (100)	0.15 (6)	0.34 ± 0.11 (12)	2.25 ± 0.88 (82)	0.76 ± 0.19 (28)	0.15 (6)	0.33 ± 0.13 (12)	0.28 ± 0.17 (10)	1.97 ± 0.77 (72)	0.00 (0)	0.00 ± 0.14 (0)	1.97 ± 0.77 (72)

[a]Values in parentheses are percentage of the total beam attenuation coefficient. Abbreviations are as follows: DR, Deep River; BSC, Big Spring Creek.

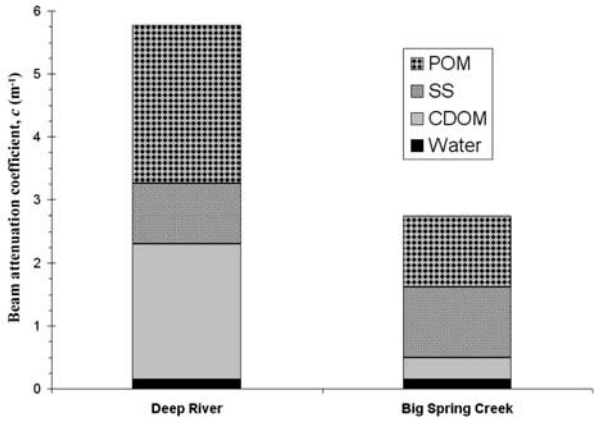

Figure 8. Component contributions to the total beam attenuation coefficient at Deep River and Big Spring Creek during base flow.

[42] The predicted product of $c_{ds}Q_{ds}$* (via equation (9)) and the actual product of $c_{ds}Q_{ds}$ (via Figure 11) agreed fairly well (Table 5). All predicted products were within 20% of the actual product, except the two uppermost confluences. These two exceptions may have been caused by the greater variability in mixing/sedimentation processes in headwater streams, and/or the greater uncertainty of Q for small watersheds. The other five confluences suggest that clarity in BR is generally volume conservative.

6. Discussion

6.1. Water Clarity in Rivers

6.1.1. Five Components

[43] Water clarity in rivers is dictated by the trends of five components: pure water, suspended sediment, particulate organic matter, chromophoric dissolved organic matter, and phytoplankton. The optical properties of pure water remain constant, and therefore its contribution to beam attenuation decreases with increases in any of the other four components. Using a wide variety of rivers, we found that water clarity is primarily dictated by the particulates in the water column rather than by dissolved constituents. Our results are similar to *Davies-Colley and Close* [1990], who analyzed 96 New Zealand rivers during base flow and found that 87% of the total light beam attenuation was attributed to particulates.

[44] Our study also showed that during floods, the dominance of c_p increases (Figure 7c) as SS and POM increase. The relative dominance of SS versus POM is likely to vary between (Figure 8) and within rivers (Figure 9a) owing to source limitations. For example, the water clarity of rivers in the Midwest USA, such as BR, that drain areas with organic-rich soils and abundant vegetation is likely to be dominated by POM; whereas, the water clarity of rivers in the Southwest USA, such as the Colorado River, that drain areas of organic-poor soils and sparse vegetation is likely to be dominated by SS.

[45] The contribution of CDOM to beam attenuation is also likely to vary between rivers (Figure 8) owing to source limitations. However, along the river continuum, CDOM typically remains fairly constant (Figure 10a) [*Smith et al.*, 1997], except in rivers with large water contributions from

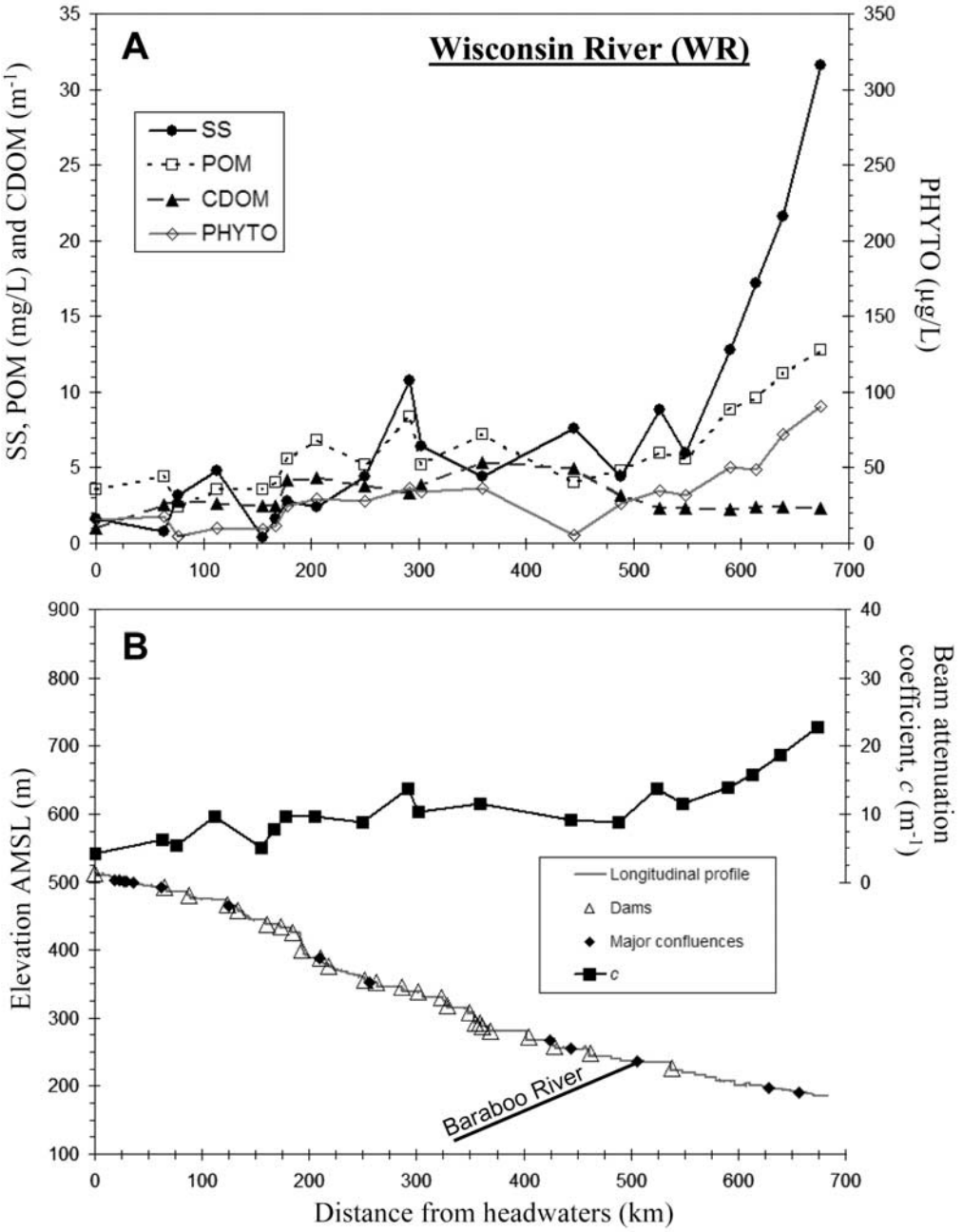

Figure 9. (a) Water chemistry and (b) longitudinal profile and beam attenuation along Wisconsin River on 16 September 2006. A major confluence is where a tributary with a stream order $\geq$ n$-$1 enters WR (n = stream order of WR before confluence).

wetlands [*Gallegos*, 2005], heavily regulated rivers such as WR (Figure 9a), and heavily disturbed rivers [*Davies-Colley*, 1987]. The temporal trends in CDOM are mostly influenced by the hydrologic regime of the river (Figure 7). Because most of the CDOM present in rivers is derived from displaced soil moisture [*Webster et al.*, 1995; *Wetzel*, 2001], the contribution of CDOM to beam attenuation is usually greater following storms and increases as particulates settle out of the water column (Figure 7c).

[46] We did not quantify c_{PHYTO}, but other riverine OWQ studies [*Davies-Colley and Close*, 1990; *Duarte et al.*, 2000; *Vahatalo et al.*, 2005] found that the contribution of PHYTO to light attenuation was either minimal or negligible over a wide range of rivers owing to unfavorable conditions for phytoplankton growth. While particulates dominate beam attenuation for most rivers, there are exceptions, most notably in tidal and blackwater rivers [e.g., *Gallegos*, 2005]. In these rivers, PHYTO and CDOM have a much greater influence on beam attenuation. Future OWQ research opportunities can be directed toward determining if trends observed here hold for diverse types of rivers worldwide.

6.1.2. Optical Water Quality Measurements

[47] Riverine optical water quality has been measured using a variety of instruments, including a beam transmissometer [*Davies-Colley and Smith*, 1992], Secchi disk

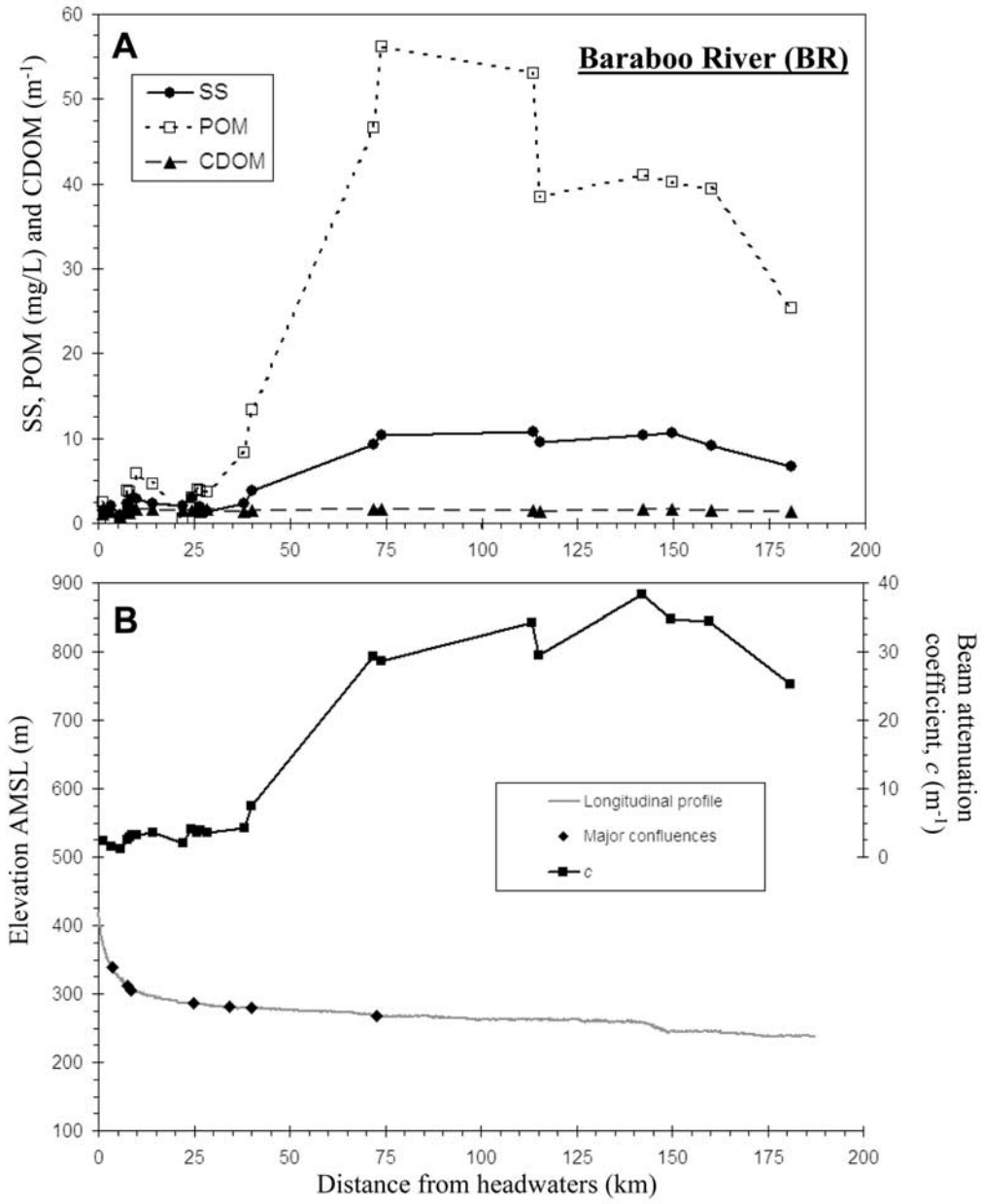

Figure 10. (a) Water chemistry and (b) longitudinal profile and beam attenuation along Baraboo River on 13 August 2006. A major confluence is where a tributary with a stream order $\geq$ n−1 enters BR (n = stream order of BR before confluence). There were no dams along BR.

[*Davies-Colley*, 1987], black disk [*Davies-Colley*, 1990], and spectrophotometer [*Vahatalo et al.*, 2005]. While each method has its advantages and disadvantages [see *Davies-Colley et al.*, 2003], we used a spectrophotometer because of its versatility. By using the four-configuration spectrophotometer scan, we were able to distinguish between absorption and scattering of both particulate and dissolved constituents. We were also able to distinguish beam attenuation between SS and POM using an empirical coefficient (b_{POM}/a_{POM}) from one of our study sites. This scattering to absorption ratio for POM will need to be further investigated over a wider range of rivers before this new method becomes practical. In addition to our compartmental method, there are other sophisticated techniques that can be used to distinguish different components of light attenuation and provide highly accurate riverine OWQ measurements [*Davies-Colley and Smith*, 1992; *Roesler*, 1998].

[48] Despite the utility and accuracy of these sophisticated methods, the time, detail, and cost involved in such analyses may not make them practical tools for water resource managers to assess riverine OWQ. We therefore recommend the use of turbidity (T_n) as a relative measure of OWQ. Comparisons of T_n and c showed that T_n is a strong predictor of water clarity (Figure 5), and data from studies of New Zealand rivers produced similar relationships [*Davies-Colley*, 1987; *Davies-Colley and Nagels*, 2008; *Davies-Colley and Smith*, 1992, 2001; *Smith et al.*, 1997]. The use of T_n as a measure of OWQ over light attenuation coefficients is advantageous because: (1) there is a longer and more extensive record of T_n in rivers (e.g., USGS water

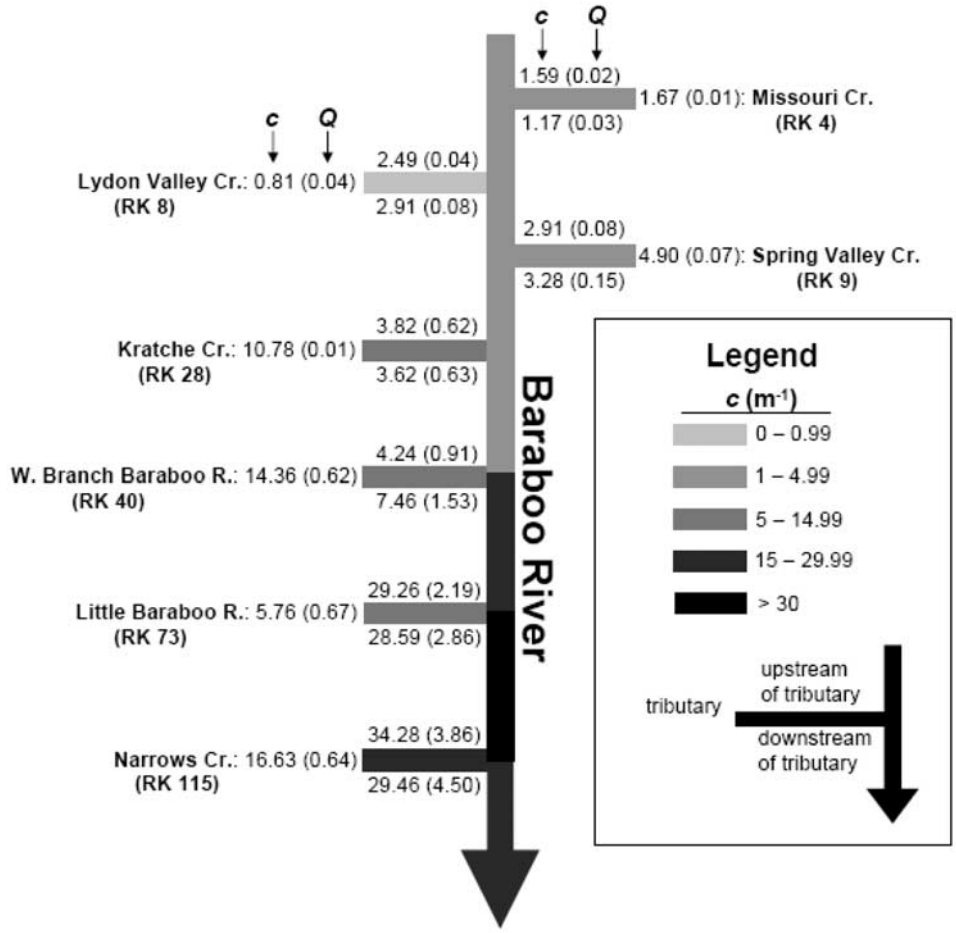

Figure 11. Water quality budget for Baraboo River. All but two of the tributaries are major tributaries (Kratche Creek and Narrows Creek). The distance of the confluence from the headwaters in km (RK) is given below its name. Schematic is not drawn to scale.

quality monitoring network); (2) T_n is easier and less expensive to measure; and (3) T_n is increasingly becoming a popular metric in fluvial ecology studies. Disadvantages of using T_n are (1) it does not use fundamental scientific units reducible to mass or length; (2) its value is instrument specific owing to different optical designs; and (3) it is not sensitive to changes in absorption [*Davies-Colley and Smith*, 2001]. Methods to overcome these limitations are to use the same instrument for all measurements (e.g., Hach 2100P) and perform an in situ calibration with a relevant optical property (e.g., Figure 5). The use of T_n as a relative measure of OWQ is probably only valid for nontidal, nonblackwater rivers where scattering is the dominant process of light attenuation [*Davies-Colley and Smith*, 2001]. In tidal and blackwater rivers, where absorption is likely to be the dominant process of light attenuation, other measures such as CDOM or *chl-a* will need to be used.

Table 5. Predicted Versus Actual Tributary Effects on Beam Attenuation in Baraboo River[a]

RK	$c_{trib}Q_{trib}$	$c_{us}Q_{us}$	$c_{ds}Q_{ds}$	$c_{ds}Q_{ds}$*	$c_{ds}Q_{ds}$*/$c_{ds}Q_{ds}$
4	0.01	0.03	0.04	0.05	1.38
8	0.03	0.10	0.23	0.13	0.56
9	0.33	0.23	0.49	0.57	1.16
28	0.15	2.34	2.28	2.50	1.10
40	8.90	3.87	11.43	12.77	1.12
73	3.86	64.18	81.85	68.03	0.83
115	10.59	132.44	132.59	143.03	1.08

[a]Here $c_{ds}Q_{ds}$* is the predicted product according to equation (9), and $c_{ds}Q_{ds}$ is the actual product according to Figure 10.

6.2. OWQ Across the Hydrograph

[49] Every study that has compared OWQ to Q, including this study, has found that water clarity decreases (c increases) exponentially with increasing Q ($c = \alpha Q^{\beta}$) due primarily to increased TSS [e.g., *Davies-Colley*, 1987, 1990; *Smith et al.*, 1997]. The rating coefficient (α) and exponent (β) are river-dependent, but in general, β is highest for rivers with large sources of readily available sediment or organic matter [*Davies-Colley*, 1990; *Davies-Colley et al.*, 1992]. The source of readily available sediment is influenced by basin geology, topography, land use, and storm frequency [*Syvitski et al.*, 2000]. Our results suggest that storm frequency is the dominant control on β. For example, even though the DR basin has more readily available sediment owing to greater relief and more intensive land use, β is higher for BSC (4.85) than DR (1.04), which we attribute to BSC's much lower storm frequency (Figure 6). The low storm frequency of its basin allows BSC to remain clear for most of the year owing to infrequent surface

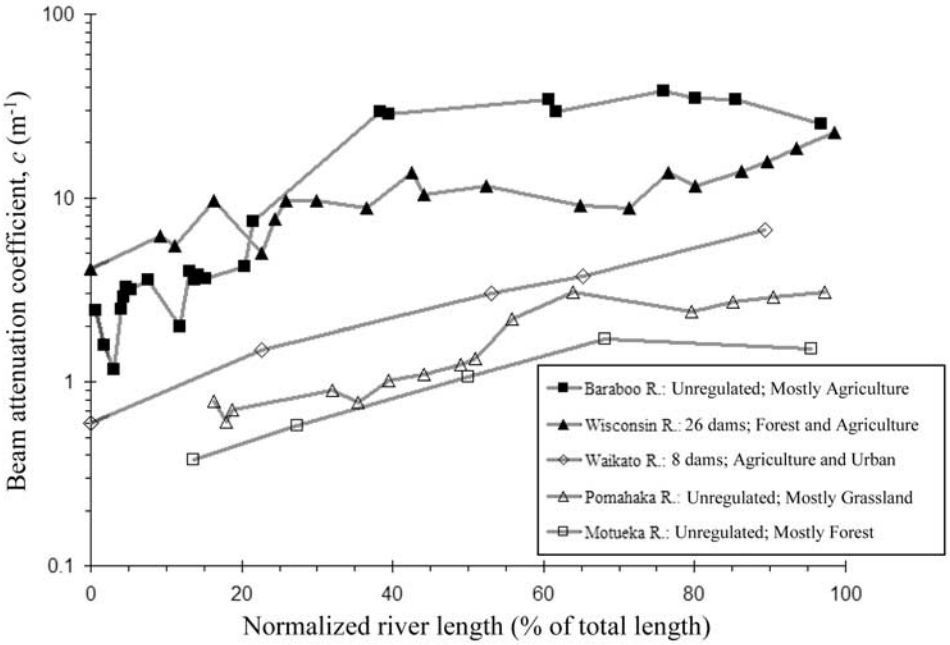

Figure 12. Water clarity along the river continuum. Degree of flow regulation and dominant land use is provided next to the name of each case study.

runoff. This infrequent surface runoff also allows more time for sources of SS and POM to accumulate, which together results in a high stormflow c to base flow c ratio (c_{sf}/c_{bf}). The higher storm frequency of the DR basin sustains elevated turbidity at base flow and also prevents large source accumulations of SS and POM, which together results in a lower c_{sf}/c_{bf}, hence a lower β. Temporal variations in OWQ can also be influenced by seasonal effects such as exposed soil surface in winter, crop harvesting, and vegetation senescence (basin-wide and in-channel).

[50] The change of c with Q is further influenced by the composition of river water. Our results from base flow and storm sampling at DR showed that POM remained in the water column longer than SS, and thus its relative role in beam attenuation increased with time following floods. We attribute this temporal trend to POM having a lower settling velocity than SS. Our study also showed that the contribution of CDOM to c increases following floods as particulates settle out of suspension and terrestrial subsurface contributions increase (Figure 7). Rivers in which PHYTO significantly influences water clarity will most likely experience diurnal and seasonal changes in c with Q owing to the response of PHYTO to sunlight and temperature [*Reynolds*, 2000]. In all, the combined effects of storm frequency, seasonality, and water chemistry are likely to produce great temporal variations in OWQ for any given river.

6.3. OWQ Along the River Continuum

[51] We now address the prediction proposed by *Vannote et al.* [1980] that water clarity decreases (c increases) along the river continuum. Of the five case studies (section 4.7), Motueka River had the least developed basin, with most of its area being forest and conservation lands [*Basher*, 2003]. Accordingly, Motueka River had the lowest c along its entire length (Figure 12). The Pomahaka basin was also relatively undeveloped with most of its land being grasslands [*Harding et al.*, 1999]. Accordingly, Pomahaka River had the second lowest c along its entire length. The Waikato River began at the outlet of Lake Taupo and thus was very clear at its headwaters. Intensive agriculture along the Waikato River caused it to become progressively more turbid [*Davies-Colley*, 1987].

[52] The average c-values along the river continuum for the two U.S. rivers were an order of magnitude higher than the NZ rivers (Figure 12), which we attribute to greater availability of organic-rich fine sediments, more aggressive agricultural practices, and poorer water quality management. Two of the five rivers had main stem dams: Waikato River (8) and Wisconsin River (26). Reservoirs tend to reduce SS, POM [*Grant et al.*, 2003] and CDOM [*Larson et al.*, 2007], and increase PHYTO [*Vahatalo et al.*, 2005], and thus are likely to disrupt spatial trends in c (Figure 9). Therefore, the three unregulated rivers, Baraboo, Pomahaka, and Motueka, provided the best case studies to analyze water clarity along the river continuum.

[53] The water clarity of the three unregulated rivers followed a similar trend, where c increased over the first 70% of the river continuum and then began to decrease (Figure 12). We suggest that this asymptotic trend, as well as the longitudinal variability of water clarity, is dictated by the channel network configuration (i.e., density and location of tributaries; *Benda et al.* [2004]). Tributaries are point sources for all five light attenuating components, and therefore confluences should be sites where changes in OWQ are most likely to occur. Baraboo River (Figures 10b and 11) provided an excellent example of confluence effects on water clarity. Between RK 20 and 40, three major tributaries entered Baraboo River, which coincided with the greatest increase in c; whereas 40 km after the last major tributary, c began to decrease. For the Pomahaka River, *Harding et al.* [1999] attributed the increase in c to

turbid inflows from tributaries draining agriculturally dominated regions. Like Baraboo River, the decrease in c over the last 30% of Pomahaka and Motueka Rivers coincided with the absence of major tributaries. This lack of major tributaries near the outlet of large rivers is consistent with the Network Dynamics Hypothesis [*Benda et al.*, 2004], which states that the distance between ''geomorphically significant tributaries'' increases with distance downstream owing to the continually reduced drainage area available in dendritic, pear-shaped basins. The decrease in c along the last 30% of the three unregulated rivers was most likely the result of a decreased supply of suspended particulates from large tributaries, and we expect a similar asymptotic trend for other dendritic, pear-shaped basins.

[54] Wisconsin River provided a counterexample to the above pattern, as five major tributaries enter the channel over its last 38% and c increased (Figure 9b). These tributary locations were a consequence of a rectangular-shaped basin providing a relatively constant available drainage area along the river's continuum (Figure 1). Major tributaries are point sources of SS and POM, which likely caused the increase in c over the last 30% of Wisconsin River (Figure 12). We therefore expect the trend of c along the river continuum to vary for different basin configurations.

[55] Our hypothesis of channel network configuration dictating OWQ shares some of the principles of the Link Discontinuity Concept (LDC) [*Rice et al.*, 2001]. The LDC states that tributaries are not just disruptions to the river continuum that temporarily reset downstream changes in physical conditions as proposed by the RCC; but rather, ''by defining patterns of water and sediment flux, they are entirely responsible for moderate- and large-scale variations in physical habitat along all river channels'' [*Rice et al.*, 2001]. Spatial patterns in water clarity are consistent with the LDC that rivers may be more appropriately viewed as a series of links, where two separate fluxes of water and sediment meet to form a new channel (equation (9)). In order to apply the LDC to optical water quality, we need to include CDOM, POM, and PHYTO fluxes as well. Applying this links concept to OWQ assumes some degree of volume conservation, which we found for Baraboo River (Figure 11 and Table 5). Volume conservation will not always apply due mainly to sedimentation, especially at headwater links [*Gomi et al.*, 2002]; but for larger rivers, we expect this mass balance approach to predict downstream water clarity within 20% (Table 5). There are also biochemical transformations that could affect volume conservation [e.g., *Moreira-Turcq et al.*, 2003], but their effect is probably negligible owing to the dominance of particulates on beam attenuation.

[56] The major limitation of the links concept for OWQ is that changes in water clarity occur in the absence of tributaries as well. Owing to the increasing contribution of particulate-free groundwater to total Q [*Leopold and Maddock*, 1953] and the increasing potential of sedimentation and hyporheic exchange processes in the downstream direction [*Packman et al.*, 2000], the absence of major tributaries typically leads to downstream decreases in c. So even though water clarity is strongly influenced by tributary inputs, the entire basin configuration must be assessed in order to develop accurate OWQ budgets for rivers.

7. Conclusion

[57] While light is recognized as a primary limiting variable in rivers, it has received comparatively limited empirical study. Water resource managers should be aware of spatial and temporal variability of OWQ as it is an important indicator of water quality change and dictates aesthetics of water resources of interest to the general public. Ecologically, light availability is likely to become an increasingly important regulator of primary production and species composition in rivers subject to greater human land use and nutrient enrichment [*Hilton et al.*, 2006]. Anthropogenic land use has also resulted in rivers with higher turbidity [*Walling and Fang*, 2003], reducing visual habitat and predation for sighted animals like fish. By knowing the controls and spatiotemporal trends of riverine OWQ, fluvial ecologists will be more able to quantify aquatic light regimes and understand consequences of light variability on multiple ecological processes. Additionally, remote sensing applications will benefit from OWQ studies as the optical characteristics of the water column must be known to derive its depth and composition from radiance measurements [*Jensen*, 2007].

[58] Most of the referenced literature in this treatise is derived from studies in New Zealand. The reason most riverine OWQ studies have been performed in New Zealand is that they have and regulate OWQ standards [see *Davies-Colley et al.*, 2003]. We advocate broad adoption of similar OWQ standards to foster ecosystem health and protect the recreational (and aesthetic) quality of waters. Designating and regulating these standards will require considerable monitoring. From a management perspective, our study suggests that tributaries should be monitored with greater frequency and extent since they are the point sources for the components that set OWQ. Further, we suggest that the abovementioned trends and concepts, particularly the role of channel network configuration, can also be used to understand the spatiotemporal trends of other water quality variables. The OWQ of rivers has greater significance because it affects receiving waters such as lakes, estuaries, and coastal environments, whose biota greatly depend on aquatic light availability, including coral [*Fabricius*, 2005], birds [*Henkel*, 2006], and submersed aquatic vegetation [*Dennison et al.*, 1993]. This study has highlighted the high spatiotemporal variability of riverine OWQ, and in doing so has opened up a number of promising research avenues including the need to understand the effects of land use and climate change on OWQ as critical steps toward a broader awareness of the fundamental role of light as a driver of multiple processes in fluvial ecosystems.

Notation

a total absorption coefficient (m^{-1}),
a_d absorption coefficient of dissolved constituents (m^{-1}),
a_p absorption coefficient of particulates (m^{-1}),
a_w absorption coefficient of pure water (m^{-1}),
a_{440} absorption coefficient at 440 nm (m^{-1}),
b total scattering coefficient (m^{-1}),
b_d scattering coefficient of dissolved constituents (m^{-1}),
b_p scattering coefficient of particulates (m^{-1}),

b_w scattering coefficient of pure water (m^{-1}),
b_{POM} scattering coefficient of particulate organic matter (m^{-1}),
c total (light) beam attenuation coefficient (m^{-1}),
c_d beam attenuation coefficient of dissolved constituents (m^{-1}),
c_p beam attenuation coefficient of particulates (m^{-1}),
c_w beam attenuation coefficient of pure water (m^{-1}),
chl-a chlorophyll-a (μg/L),
y_{BD} black disk visibility distance (m),
z_{SD} Secchi disk visibility depth (m),
AMSL above mean sea level,
BSC Big Spring Creek,
BR Baraboo River,
CDOM chromophoric dissolved organic matter (a_{440} index),
D absorbance ($\log_{10}\ \Phi_0/\Phi$),
DOC dissolved organic carbon (mg/L),
DR Deep River,
F filtered water sample,
IOP inherent optical property,
K b_{POM}/a_{POM},
OWQ optical water quality,
Φ_0 incident radiant flux (mol/s),
Φ transmitted radiant flux (mol/s),
PHYTO phytoplankton (μg/L),
POM particulate organic matter (mg/L),
Q discharge or volume of water per time (m^3/s),
Q_{peak} maximum discharge during a flood (m^3/s),
Q_{ds} discharge of river just downstream of a tributary (m^3/s),
Q_{trib} discharge of tributary just before confluence with main stem (m^3/s),
Q_{us} discharge of river just downstream of a tributary (m^3/s),
SCH standard cell holder; used to obtain a,
SS suspended sediment (mg/L),
T_n turbidity (NTU),
TCH turbidity cell holder; used to obtain c,
TSS total suspended solids (mg/L),
UF unfiltered water sample,
X apparent absorption coefficient (m^{-1}),
WR Wisconsin River.

[59] **Acknowledgments.** This project was supported by the National Research Initiative of the USDA Cooperative State Research, Education, and Extension Service (CSREES grant 2004-35102-14793) and NSF grant DEB-0321559. Additional support was provided by U.S. Fish and Wildlife Service and Restoration Systems, LLC. A portion of laboratory resources were provided by Stephen C. Whalen and Robert G. Wetzel. Special thanks to Bill Ginsler and the town of Big Spring, Wisconsin, for site access. Richelle Baroudi, Zack Feiner, Victoria Julian, Ryan Kroiss, Mark Lochner, Steve Neary, Hollis Rhinelander, Matt Smith, Leah Vandenbusch, Sally Whisler, and Sarah Zahn assisted with field and laboratory work. This manuscript benefited greatly from reviews by Rob Davies-Colley and two anonymous reviewers.

References

Babin, M., and D. Stramski (2004), Variations in the mass-specific absorption coefficient of mineral particles suspended in water, *Limnol. Oceanogr.*, *49*, 756–767.

Basher, L. R. (2003), The Motueka and Riwaka catchments: A technical report summarising the present state of knowledge of the catchments, management issues and research needs for integrated catchment management, 122 pp., Manaaki Whenua Landcare Res., Lincoln, Neb.

Benda, L., et al. (2004), The network dynamics hypothesis: How channel networks structure riverine habitats, *BioScience*, *54*, 413–427, doi:10.1641/0006-3568(2004)054[0413:TNDHHC]2.0.CO;2.

Bricaud, A., et al. (1983), Optical efficiency factors of some phytoplankters, *Limnol. Oceanogr.*, *28*, 816–832.

Buiteveld, H., et al. (1994), The optical properties of pure water, paper presented at SPIE Ocean Optics XII, Bergen, Norway, 13–15 June.

Clesceri, L. S., A. E. Greenberg, and A. D. Eaton (1998), *Standard Methods for the Examination of Water and Wastewater*, 20th ed., Am. Public Health Assoc., Washington, D. C.

Davies-Colley, R. J. (1987), Optical properties of the Waikato River, New Zealand, *Mitt. Geol. Palaontol. Inst. Univ. Hamburg SCOPE/UNEP Sonderband*, *64*, 443–460.

Davies-Colley, R. J. (1988), Measuring water clarity with a black disk, *Limnol. Oceanogr.*, *33*, 616–623.

Davies-Colley, R. J. (1990), Frequency distributions of visual water clarity in 12 New Zealand rivers, *N. Z. J. Mar. Freshwater Res.*, *24*, 453–460.

Davies-Colley, R. J., and M. E. Close (1990), Water colour and clarity of New Zealand rivers under baseflow conditions, *N. Z. J. Mar. Freshwater Res.*, *24*, 357–365.

Davies-Colley, R. J., and J. W. Nagels (2008), Predicting light penetration into river waters, *J. Geophys. Res.*, *113*, G03028, doi:10.1029/2008JG000722.

Davies-Colley, R. J., and D. G. Smith (1992), Offsite measurement of the visual clarity of waters, *Water Resour. Bull.*, *28*, 951–957.

Davies-Colley, R. J., and D. G. Smith (2001), Turbidity, suspended sediment, and water clarity: A review, *J. Am. Water Resour. Assoc.*, *37*, 1085–1101, doi:10.1111/j.1752-1688.2001.tb03624.x.

Davies-Colley, R. J., et al. (1992), Effects of clay discharges on streams: 1. Optical properties and epilithon, *Hydrobiologia*, *248*, 215–234, doi:10.1007/BF00006149.

Davies-Colley, R. J., et al. (2003), *Colour and Clarity of Natural Waters*, 310 pp., Ellis Horwood, New York.

Dennison, W. C., et al. (1993), Assessing water-quality with submersed aquatic vegetation, *BioScience*, *43*, 86–94, doi:10.2307/1311969.

Duarte, C. M., et al. (2000), Particulate light absorption and the prediction of phytoplankton biomass and planktonic metabolism in northeastern Spanish aquatic ecosystems, *Can. J. Fish. Aquat. Sci.*, *57*, 25–33, doi:10.1139/cjfas-57-1-25.

Fabricius, K. E. (2005), Effects of terrestrial runoff on the ecology of corals and coral reefs: Review and synthesis, *Mar. Pollut. Bull.*, *50*, 125–146, doi:10.1016/j.marpolbul.2004.11.028.

Gallegos, C. L. (2005), Optical water quality of a blackwater river estuary: The Lower St. Johns River, Florida, USA, *Estuarine Coastal Shelf Sci.*, *63*, 57–72, doi:10.1016/j.ecss.2004.10.010.

Gallegos, C. L., and P. J. Neale (2002), Partitioning spectral absorption in case 2 waters: Discrimination of dissolved and particulate components, *Appl. Opt.*, *41*, 4220–4233, doi:10.1364/AO.41.004220.

Golladay, S. W. (1997), Suspended particulate organic matter concentration and export in streams, *J. N. Am. Benthol. Soc.*, *16*, 122–131, doi:10.2307/1468245.

Gomi, T., et al. (2002), Understanding processes and downstream linkages of headwater systems, *BioScience*, *52*, 905–916, doi:10.1641/0006-3568(2002)052[0905:UPADLO]2.0.CO;2.

Gordon, H. R., and A. W. Wouters (1978), Some relationships between Secchi depth and inherent optical properties of natural waters, *Appl. Opt.*, *17*, 3341–3343.

Gordon, N. D., et al. (2004), *Stream Hydrology: An Introduction for Ecologists*, 429 pp., John Wiley, Hoboken, N. J.

Grant, G. E., et al. (2003), A geological framework for interpreting downstream effects of dams on rivers, in *A Peculiar River: Geology, Geomorphology, and Hydrology of the Deschutes River, Oregon* edited by J. E. O'Connor and G. E. Grant, pp. 209–225, AGU, Washington, D. C.

Harding, J. S., et al. (1999), Changes in agricultural intensity and river health along a river continuum, *Freshwater Biol.*, *42*, 345–357, doi:10.1046/j.1365-2427.1999.444470.x.

Hauer, F. R., and G. A. Lamberti (1996), *Methods in Stream Ecology*, 674 pp., Elsevier, New York.

Henkel, L. A. (2006), Effect of water clarity on the distribution of marine birds in nearshore waters of Monterey Bay, California, *J. Field Ornithol.*, *77*, 151–156, doi:10.1111/j.1557-9263.2006.00035.x.

Hilton, J., et al. (2006), How green is my river? A new paradigm of eutrophication in rivers, *Sci. Total Environ.*, *365*, 66–83, doi:10.1016/j.scitotenv.2006.02.055.

Jensen, J. R. (2007), *Remote Sensing of the Environment: An Earth Resource Perspective*, 592 pp., Prentice-Hall, Upper Saddle River, N. J.

Kirk, J. T. O. (1988), Optical water quality—What does it mean and how should we measure it? J, *Water Pollut. Control Fed.*, *60*, 194–197.

Kirk, J. T. O. (1994), *Light and Photosynthesis in Aquatic Ecosystems*, 509 pp., Cambridge Univ. Press, New York.

Larson, J. H., et al. (2007), Effects of upstream lakes on dissolved organic matter in streams, *Limnol. Oceanogr.*, *52*, 60–69.

Leopold, L. B., and T. Maddock Jr. (1953), The hydraulic geometry of stream channels and some physiographic implications, *U. S. Geol. Surv. Prof. Pap.*, *252*, 1–57.

Moreira-Turcq, P. F., et al. (2003), Characteristics of organic matter in the mixing zone of the Rio Negro and Rio Solimoes of the Amazon River, *Hydrol. Process.*, *17*, 1393–1404, doi:10.1002/hyp.1291.

Packman, A. I., et al. (2000), A physicochemical model for colloid exchange between a stream and a sand streambed with bed forms, *Water Resour. Res.*, *36*, 2351–2361, doi:10.1029/2000WR900059.

Petzold, T. J. (1972), *Volume scattering functions for selected ocean waters*, 79 pp., Visibility Lab., Scripps Inst. of Oceanogr., San Diego, Calif.

Popp, A. S. (2005), Longitudinal patterns of carbon, chlorophyll, and nutrients in the Wisconsin River, M. S. thesis, Univ. of Wis., Madison, Wis.

Reynolds, C. S. (2000), Hydroecology of river plankton: The role of variability in channel flow, *Hydrol. Process.*, *14*, 3119–3132, doi:10.1002/1099-1085(200011/12)14:16/17<3119::AID-HYP137>3.0.CO;2-6.

Rice, S. P., et al. (2001), Tributaries, sediment sources, and the longitudinal organisation of macroinvertebrate fauna along river systems, *Can. J. Fish. Aquat. Sci.*, *58*, 824–840, doi:10.1139/cjfas-58-4-824.

Roesler, C. S. (1998), Theoretical and experimental approaches to improve the accuracy of particulate absorption coefficients derived from the quantitative filter technique, *Limnol. Oceanogr.*, *43*, 1649–1660.

Sedell, J. R., and C. N. Dahm (1990), Spatial and temporal scales of dissolved organic carbon in streams and rivers, in *Organic Acids in Aquatic Ecosystems*, edited by E. M. Perdue and E. T. Gjessing, pp. 261–279, John Wiley, Hoboken, N. J.

Smith, D. G., et al. (1997), Optical characteristics of New Zealand rivers in relation to flow, *J. Am. Water Resour. Assoc.*, *33*, 301–312, doi:10.1111/j.1752-1688.1997.tb03511.x.

Syvitski, J. P., et al. (2000), Estimating fluvial sediment transport: The rating parameters, *Water Resour. Res.*, *36*, 2747–2760, doi:10.1029/2000WR900133.

Vahatalo, A. V., et al. (2005), Light absorption by phytoplankton and chromophoric dissolved organic matter in the drainage basin and estuary of the Neuse River, North Carolina (USA), *Freshwater Biol.*, *50*, 477–493, doi:10.1111/j.1365-2427.2004.01335.x.

Vannote, R. L., et al. (1980), The river continuum concept, *Can. J. Fish. Aquat. Sci.*, *37*, 130–137.

Walling, D. E., and D. Fang (2003), Recent trends in the suspended sediment loads of the world's rivers, *Global Planet. Change*, *39*, 111–126, doi:10.1016/S0921-8181(03)00020-1.

Walling, D. E., and B. W. Webb (1992), Water quality: I. Physical characteristics, in *The Rivers Handbook: Hydrological and Ecological Principles*, edited by P. Calow and G. E. Petts, pp. 48–72, Blackwell Sci., Malden, Mass.

Webster, J. R., et al. (1995), Organic processes in streams of the eastern United States, in *River and Stream Ecosystems*, edited by C. E. Cushing et al., pp. 117–187, Elsevier, New York.

Wetzel, R. G. (2001), *Limnology: Lake and River Ecosystems*, 1006 pp., Elsevier, New York.

Wetzel, R. G., and G. E. Likens (2000), *Limnological Analyses*, 3 ed., 429 pp., Springer, New York.

Zahn, S. E. (2007), Submerged macrophytes in Big Spring Creek, WI: Distribution and influence on phosphorous dynamics, 29 pp., B. S. thesis, Univ. of Wis., Madison, Wis.

M. W. Doyle, Department of Geography, University of North Carolina, 205 Saunders Hall, Chapel Hill, NC 27599-3229, USA. (mwdoyle@email.unc.edu)

J. P. Julian, Department of Geography, University of Oklahoma, 100 East Boyd Street, SEC Suite 684, Norman, OK 73019, USA. (jjulian@ou.edu)

S. M. Powers and E. H. Stanley, Center for Limnology, University of Wisconsin, 680 North Park Street, Madison, WI 53706, USA. (smpowers@wisc.edu; ehstanley@wisc.edu)

J. A. Riggsbee, Department of Environmental Sciences and Engineering, University of North Carolina, 166 Rosenau Hall, Chapel Hill, NC 27599, USA. (ariggsbee@restorationsystems.com)